

Realize Better Risk Characterization of STHE Tube Failure Scenarios Through Relief Systems Dynamics Modeling

An ioMosaic Corporation White Paper



G. A. Melhem, Ph.D.

melhem@iomosaic.com

This page intentionally left blank

IOMOSAIC CORPORATION

Relief and Flare Systems Design and Evaluation Practices

Heat Exchangers

*Realize Better Risk Characterization of STHE Tube Failure
Scenarios Through Relief Systems Dynamics Modeling*

authored by

Georges A. MELHEM, Ph.D., FAIChE

January 11, 2018

This page intentionally left blank

Contents

1 Abstract	3
2 Tube Failure Mechanisms and Geometry	4
2.1 Additional Considerations	5
3 Tube Failure Frequency	5
4 High Pressure Ethylene Example	7
5 Speed of Sound Considerations	8
6 Tube Failure Flow Rates	8
6.1 Ethylene STHE - Tube Rupture Flow Rates	9
7 Moving Shocks	10
8 Surge Pressure Caused by High Pressure Fluid	13
8.1 Gas Flow Striking a Liquid	15
8.2 Liquid Flow Striking a Liquid	17
8.3 Two-Phase and/or Non-Ideal Fluid Flow Striking a Liquid	17
9 Reaction Forces	18
9.1 Example	20
9.2 The Use of Dynamic Load Factors	21
10 Structural Loads Following Tube Failure	22
10.1 (a) Shell Side Liquid Acceleration Forces	22
10.1.1 Initially Liquid Full Relief Discharge Piping	23
10.2 (b) Relief Piping Transient Liquid Reaction Forces	25
10.2.1 Rupture Disk	25
10.2.2 Pressure Relief Valve	25
10.3 (c) Relief Piping Steady State Liquid Reaction Forces	26
10.4 Ethylene STHE - Shell Side Liquid Acceleration Forces	26

<i>CONTENTS</i>	2
11 Relief Systems Design and Evaluation	28
11.1 A - Relief Piping Transient Reaction Forces from Initial Liquid Flow	29
11.1.1 10 ft Segment	29
11.1.2 60 ft segment	29
11.2 B - Quasi-Dynamic Two-Phase Flow	29
11.3 C - Required Rupture Disk Size	33
12 SuperChems Expert Guidance	33
13 Conclusions	35
14 Appendix A - Shell Side High Pressure Condition	36

1 Abstract

The risks of shell and tube heat exchanger (STHE) sudden tube failure scenarios are often considered in relief and flare systems design and evaluation. Scenarios involving the release of high pressure gas following a sudden tube failure, especially where the shell is filled with liquids, require the use of relief and flow dynamics for better understanding of and assessment of risks, risk reduction, and relief requirements.

Historically in most existing STHE installations, the shell side of the STHE was typically protected with a rupture disk where the design basis is all vapor flow allowing for the expansion of gas from the tube pressure to the set point of the rupture disk. Rupture disks were favored over pressure relief valves because they were assumed to have faster opening and response time to the pressure wave experienced by the liquid following the tube failure.

Recent field work by the Energy Institute [1, 2] confirms that the all vapor relief requirements are not sufficient to protect the shell from deformation and potential failure. Furthermore, this recent field work also confirms that STHE shell may also be effectively protected with pressure relief valves since the measured opening time for PRVs can be on the order of 5 milliseconds while many non-fast acting rupture disk opening times can be as long as 100 milliseconds. Additional findings by the Energy Institute indicate that a reasonable tube failure frequency to consider for risk assessments and design is 1/1000 years.

Following the sudden rupture of one tube, between 0.2 and 0.7 milliseconds, high pressure gas will impact the liquid creating a shock with a duration that depends on the length of the heat exchanger shell and the speed of sound in the liquid within the shell. Small amounts of gas present in the liquid shell can temper the magnitude of this initial shock pressure. Once the pressure wave had enough time to be reflected back to the tube failure source/location, high pressure gas will expand into the shell and will cause liquid displacement through the relief device. The relief device will have to have enough capacity to expel enough liquid to create sufficient expansion volume for the high pressure gas. After a brief duration of liquid flow, two-phase flow begins. Finally, all vapor flow occurs. While this entire quasi-dynamic flow time may be on the order on 1 or 2 minutes, the static pressures developed in the shell can cause deformation and potential failure. While relief requirements are typically driven by the two-phase flow regime the relief piping structural support requirements may be driven by the transient reaction force experienced by the piping during the initial acceleration of the first liquid to be vented (slug loading).

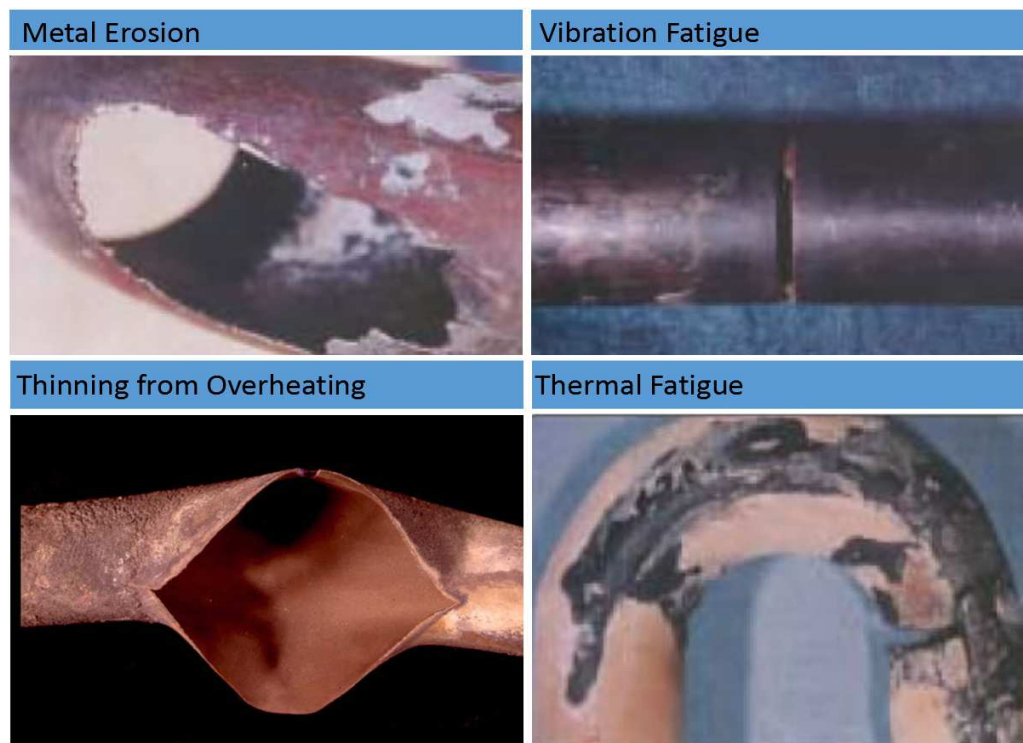
Dynamic relief systems modeling with SuperChems component of Process Safety Office can provide a lot of insight into the risks and the proper design for this scenario. In many instances, the STHE may not be blocked in during the tube failure and relief through the process line is possible in addition to the relief systems flow path. During a worst case scenario where tube failure occurs and the STHE is blocked in, relief systems dynamics can provide a prudent estimate of the pressure reached in the shell with the existing relief device and if that level of pressure can lead to deformation or potential failure. Potential failure is typically considered if the Hoop stress exceeds 2/3 the UTS at the mixed fluid final temperature with consideration of corrosion allowances for new designs or corroded thickness and remaining life for existing designs. Relief systems dynamics modeling provides a clear assessment of consequence vs. failure frequency considering other layers of protection. Such practical analysis enables operating companies to better judge the

risk, to define better risk reduction options, and to prioritize when risk reduction measures (if any) can be implemented effectively without creating additional risks for poorly planned or emergency shutdowns.

2 Tube Failure Mechanisms and Geometry

It is customary to assume that heat exchanger tube failure is likely to occur at the back side of the tube sheet leading to flow from a short tube stub remaining in the tube sheet and also through a longer section of the tube. The actual tube failure is more likely to be a longitudinal tear from a location where mechanical or corrosion damage has occurred [1, 3]. A sharp guillotine break is not likely. Tube failures take on a variety of shapes and the resulting flow area is not ideal as illustrated in Figure 1 showing typical tube failures [4].

Figure 1: Typical heat exchanger tube failures



Mechanisms associated with heat exchanger tube failure are complex. They include (a) acoustic resonance caused by complex fluid flow patterns across the tube bundle, (b) heat exchanger geometry, (c) poor selection of construction materials, and (d) fabrication techniques. Poor or inadequate inspection programs can also be an important factor.

Heat exchanger material defects caused by welding, corrosion, and erosion contribute to tube failure. Complex fluid flow patterns can give rise to vortex shedding, fluid-elastic excitation, and turbulent buffeting. Acoustic resonance can take place when the frequency of vortex shedding around

the tubes equals and couples with the natural structural frequency of the tubes leading to the conversion of mechanical kinetic energy of the fluid into damaging pressure fluctuations/pulsations.

The extent and magnitude of vibration damage can be linked to the length of the unsupported tube length, collision damage, damage caused by baffles, and tube-to-tube sheet clamping effects. Large amplitudes of vibrating tubes can cause collision damage where the tubes expand, mostly at mid-section, hitting other tubes and shell wall. As a result, they thin at the point of contact. The vibrating tubes can also hit baffles causing thinning at the baffle contact points. The tube-to-tube sheet clamping effect (tubes are expanded to tube sheet to minimize crevice) is caused by the increase in the natural frequency of vibration in the tube section adjacent to tube sheet and the increase in stress at the point where the tube emerges from the tube sheet.

Typical tube failure regions include (a) U-bends - outer rows have lower natural frequency, and are more susceptible to damage, (b) nozzle entrance and leaving areas, (c) tube sheet regions - unsupported span, (d) baffle regions - tubes located in baffle windows, and (e) obstructions tie-rods, impingement plates, sealing strips.

2.1 Additional Considerations

Tube failure has to be considered even if the tube side and shell side have the same design pressures. The impact of a tube failure on piping and other components tied into the low pressure side of the heat exchanger should also be considered. Connected equipment can experience pressures as high as the low pressure side of the heat exchanger experiences. Tube failure could place such equipment at risk. Backflow of process fluids into utility distribution systems should be prevented. Therefore, the low pressure side relief system should be designed for the entire flow from the high pressure side. In general, credit for flow out of the exchanger on the low pressure side should not be taken.

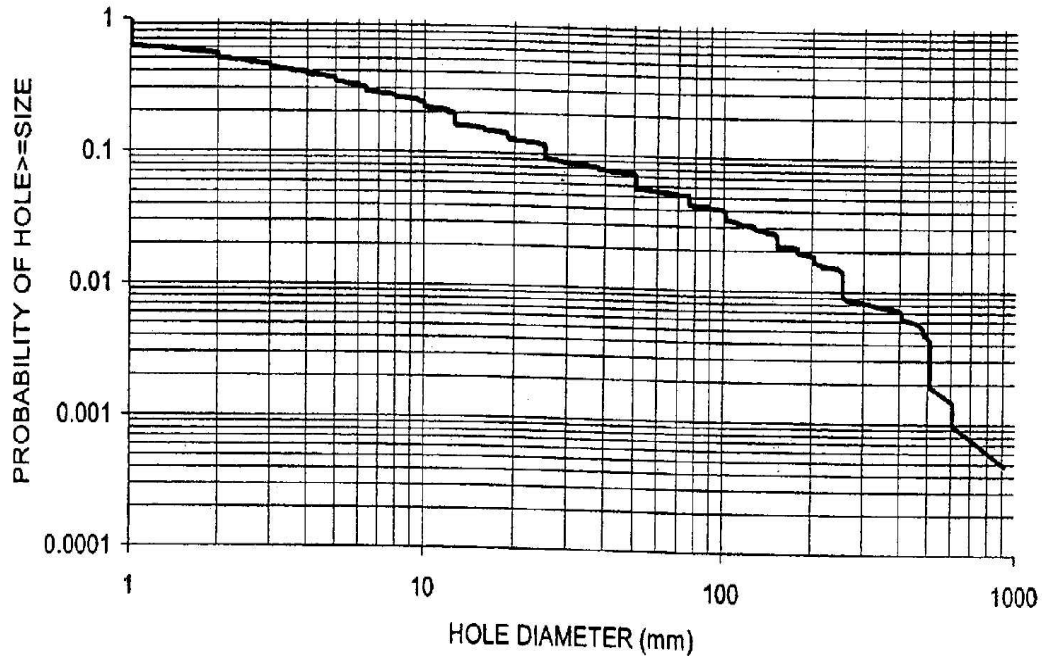
Leaks of materials from tubes may not be chemically compatible with materials on the shell side causing runaway reactions. Rapid phase transitions should also be considered when the fluid temperature difference is significant between the tube side and shell side fluids. In addition, If the gas pressure is high enough, expansion cooling to the low pressure side minimum operating pressure can result in cold temperatures that can be less than the minimum design metal temperature of the tube material causing a typical leak to progress to a catastrophic tube rupture.

3 Tube Failure Frequency

A best estimate of a sudden full bore tube failure frequency is approximately 9/10,000 years [1, 2] for one STHE. This frequency is likely to be higher if the gas flow in the tubes exceeds 50 % of the gas speed of sound due to increased vibration risk fatigue failures. In general, most tube failures are caused by corrosion and thinning of the tube metal.

Leak frequencies vary with hole size [5] and are shown to follow a frequency distribution function

Figure 2: Typical Leak size distribution, HSE offshore data [5]



that depends on equipment diameter, D , and hole size, $d \geq 1$ mm:

$$F(d) = f(D)d^m + F_r \quad (1)$$

where $F(d)$ is the failure frequency per year for holes exceeding d , $f(D)$ is the function representing the variation of leak frequency with D , m is the slope parameter, and F_r is the residual additional frequency for rupture per year. F_r and m are assumed to be constant and not dependent on equipment size for any equipment. The frequency distribution function is similar to an F/N curve where the probability of a hole size greater or equal to a specific size is obtained as a function of hole size as shown in Figure 2.

Typically the probability of a hole size range is calculated from Equation 1. In this case the rupture frequency cancels out. For example, from Figure 2 the probability of having a hole size ≥ 70 mm is 0.05/yr and the probability of having a hole size ≥ 100 mm is 0.04/yr. Therefore, the probability of having a hole size ranging from 70 to 100 mm is $0.05 - 0.04 = 0.01$ /yr.

Spouge [5] provides a generic failure frequency function for full leaks where a leak is consistent with or greater than a leak at the operating pressure:

$$F(d) = 8 \times 10^{-6} \left(1 + \frac{1000}{D^{1.3}} \right) \frac{1}{d^{1.42}} \quad (2)$$

Generic failure frequencies are typically adjusted using a management systems evaluation factor and an equipment modification factor as recommended by API-581 [6].

If we assume our tube leaks follow the same frequency function where a full rupture has a fre-

quency of 9/10,000 years, $F(d)$ will be given by:

$$F(d) = a \left(1 + \frac{1000}{D^{1.3}} \right) \frac{1}{d^{1.42}} \quad (3)$$

where a is calculated from the tube diameter for full rupture, D :

$$a = \frac{9 \times 10^{-4}}{\left(1 + \frac{1000}{D^{1.3}} \right) \frac{1}{D^{1.42}}} \quad (4)$$

Spouge [5] reports generic failure frequencies for tube leaks of 10^{-3} /year for leak diameters greater or equal to 1 mm and 4.9×10^{-5} /year for leak diameters greater or equal to 50 mm.

4 High Pressure Ethylene Example

The concepts developed in this paper will be illustrated using a STHE of high pressure ethylene gas on the tube side and cooling water on the low pressure shell side. The high-pressure side maximum operating pressure of 2,500 psig exceeds the low pressure side design pressure of 285 psig. The gas in the tubes enters at 110 F and exits at 95 F. The cooling water on the shell side is at ambient temperature, assume 80 F. The shell side was hydro tested at 428 psig. If we correct that hydro test pressure to a maximum operating shell fluid temperature of 130 F, the hydro test pressure can be derated to 410 psig.

If tube failure occurs, it is expected at the backside of the tubesheet. As a result, the flow from the high-pressure side to the low-pressure side should be modeled as (a) the flow through the U-tube and (b) the short tube stub remaining in the tubesheet. For use in the dynamic simulations, the flow through these paths is calculated as a function of built-up pressure in the low-pressure side. Other normal process flow in and out of the exchanger is assumed to stop. The tubes are 0.75 in outside diameter with a 0.109 in wall thickness leading to a tube internal diameter of 0.532 in. The tube stub remaining in the tubesheet is 4 in long and the tube length remaining in the shell is 356 inches long. There are a total of 250 tubes.

The shell operates at 110 psig and has an inside diameter of 24.375 inches and a wall thickness of 0.25 in. The length of the shell is 360 inches. The portion of the flow area of the shell that is not occupied by tubes is 76.3 % or 356 in². The speed of sound in water at ambient conditions is specified at 1,480 m/s, uncorrected for the shell flexibility. Assume the shell steel properties are well represented by a density of 7,800 kg/m³ and a modulus of elasticity of 200 GPa.

The shell side is equipped with a relief system. The relief system is a 2 inch NPS rupture disk ($K_R = 0.24$) set at 255 psig. The relief discharge piping consists of one foot 2 inch NPS horizontal inlet line, followed by a 4 inch NPS vertical 10 ft discharge segment which is followed by by a 6 inch NPS horizontal 60 ft discharge segment. Assume that the rupture disk maximum opening pressure is 5 % more than the actual or 268 psig.

5 Speed of Sound Considerations

Many of the equations used in this paper utilize the isentropic speed of sound, c_s , for establishing key design parameters such as the incident pressure/shock or the duration of the incident pressure/shock. The motion of the pipe wall can influence this value and should be considered for piping containing liquids as shown by Melhem [7]. In general the following equation can be used with reasonable accuracy regardless for all piping configurations:

$$c_e = c_s \eta = c_s \frac{1}{\sqrt{1 + \frac{E_f}{E_{solid}} \frac{d}{\delta}}} = c_s \frac{1}{\sqrt{1 + \left(\frac{c_s}{c_{s,solid}}\right)^2 \left(\frac{\rho}{\rho_{solid}}\right) \left(\frac{d}{\delta}\right)}} \quad (5)$$

As long as the wall thickness is at least 1 % of the diameter (thick pipe), or the pipe is rigid, then the motion of the tube wall does not influence the wave propagation speed of the fluid for all commercial steel pipe and tubing components. Where the value of η is less than 1, the value of c_e should be used instead of c_s .

6 Tube Failure Flow Rates

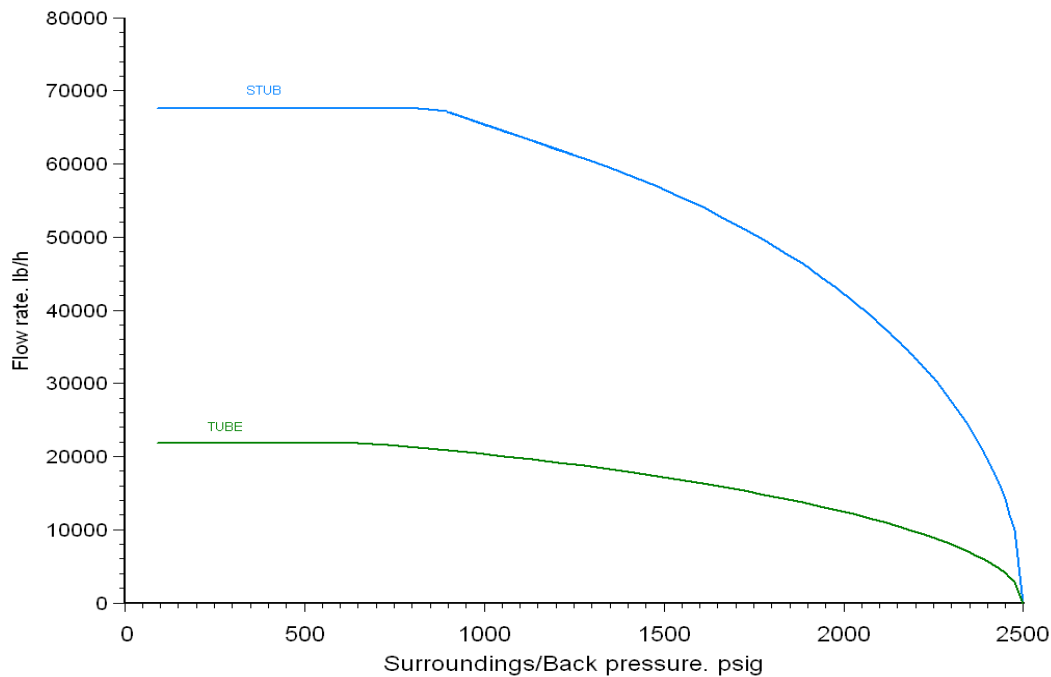
High pressure gas or two-phase flow rates from a tube failure can be calculated with reasonable accuracy from well established fluid flow models such as SuperChems Expert or SuperChems for DiERS. A prudent estimate of flow rate can be obtained from an ideal nozzle flow model using twice the flow area of a single tube and a discharge coefficient ranging from 0.62 to 0.975 for most applications. A best estimate of the flow rate can be obtained by calculating flow using a suitable pipe flow model for a short tube stub remaining in the tube sheet and the longer portion of the tube in the shell.

Moody [8] (see Pages 440 to 441) shows that the initial discharge rate from a sudden tube rupture is approximately 60 % of the actual steady state critical flow rate for an ideal gas with a heat capacity ratio γ of 1.4:

$$\frac{G_{init}}{G_c} = \frac{\sqrt{\gamma P_o \rho_o} \left(\frac{2}{\gamma+1}\right)^{\frac{\gamma+1}{\gamma-1}}}{\sqrt{\gamma P_o \rho_o} \left(\frac{2}{\gamma+1}\right)^{\frac{\gamma+1}{\gamma-1}}} = \left(\frac{2}{\gamma+1}\right)^{\frac{\gamma+1}{2(\gamma-1)}} = 0.833^3 \approx 0.58 \quad (6)$$

Where G_c is the ideal gas steady state mass flux and G_{init} is the ideal gas initial mass flux. Therefore the selection of a discharge coefficient of 0.62 with an ideal nozzle flow estimate should be reasonable for the determination of the peak transient pressure value. Best flow rate estimates using pipe flow should be used for the quasi-dynamic portion of the analysis dealing with relief sizing and dynamic and steady state reaction loads for the assessment of relief piping supports. Note the ideal gas assumption may not be suitable for high pressure systems.

Figure 3: Calculated ethylene flow from long portion and short portion of tube



6.1 Ethylene STHE - Tube Rupture Flow Rates

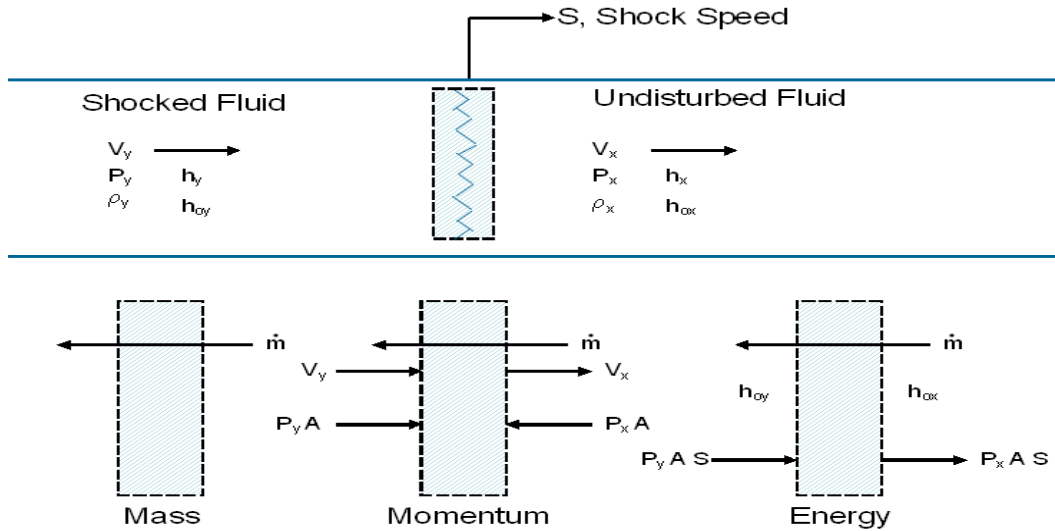
The preferred method for calculating the flow rate from the tube rupture is to use pipe flow from each end of the ruptured tube:

- L This is 4 inches long with a pressure of 2,500 psig and a temperature of 95 F.
- R This is 356 inches long with a pressure of 2,500 psig and a temperature of 110 F.

Figure 3 shows the calculated flow rate of ethylene from the long and short portions of one tube as a function of shell backpressure. We note that the flow is choked at 663 psig and 42 F for the long portion and 680 psig and 44 F for the stub with a total combined flow capacity of 89,500 lbs/hr. The calculations assume 1/2 velocity head loss for pipe entrance, and one exit loss for each portion of the ruptured tube. It is important to establish the reduction in flow as a function of backpressure for use in the quasi-dynamic portion of the analysis as liquid is vented from the shell side and pressure is increasing in the shell side due to the expansion of the incoming high pressure fluid. Note these choke points are at the two-phase boundary for ethylene indicating that condensation is occurring at the choke point and at lower backpressures. In order to simplify the presentation of results for peak incident pressure calculations, we will isentropically mix both flow contributions to a pressure of 680 psig.

Alternatively, if an ideal nozzle model was used to calculate the flow from twice the area of the ruptured tube starting at 110 F and 2500 psig, choke conditions of 652 psig and 42 F are calculated and a total flow rate of 117,400 lbs/hr at a discharge coefficient of 0.62 where the choking conditions are at the two-phase boundary. These estimates assume isentropic flow in comparison

Figure 4: Moving Normal Shock, General Fluid



with constant stagnation enthalpy flow for a pipe solution. As a result, the nozzle estimate yields a lower temperature and a higher flow rate and would lead to a more conservative assessment of the peak incident pressure for the shell side.

7 Moving Shocks

Many problems and designs of interest in fluid mechanics, such as pressure relief design, require the estimate of maximum shock pressures and velocities caused by the sudden opening of a relief device or the sudden opening/closure of a valve. Moving shock properties for a general fluid can be easily obtained using thermodynamics and fluid mechanics. A valve opening/closing time is considered to be sudden or instantaneous, if the time required to close or open the valve is small compared to the characteristic pipe period:

$$t_{open} \frac{c_e}{L_p} \ll 1.0 \text{ or } t_{open} \ll \frac{L_p}{c_e} \tag{7}$$

where c_e is the effective isentropic speed of sound in the fluid/pipe system, L_p is the flow path length, and t_{open} is the valve opening or closing time.

Let's consider a shock discontinuity moving to the right at a shock speed S as illustrated in Figure 4. The subscript x refers to the undisturbed fluid and the subscript y refers to the shocked fluid. A shock travels in a fluid at the speed of sound relative the fluid. If the fluid is traveling at velocity u ,

then:

$$S - u = c_S \text{ or } S = u + c_S \quad (8)$$

We can write mass, momentum, energy, and PVT balances across the shock as follows:

Mass

$$\dot{m} = \rho_y A_p (S - u_y) = \rho_x A_p (S - u_x) \quad (9)$$

Momentum

$$\dot{m} (u_y - u_x) = (P_y - P_x) A_p \quad (10)$$

Energy

$$\dot{m} (h_{o,y} - h_{o,x}) + (P_x - P_y) A_p S = 0 \quad (11)$$

PVT

$$\rho_y = f(P_y, T_y, x_{i,y}) \quad (12)$$

Boundary Condition

$$h_{o,y} = h_y + \frac{u_y^2}{2} \quad (13)$$

Given the initial conditions of the undisturbed fluid T_x , P_x , u_x , ρ_x , $h_{o,x}$, and the boundary conditions for the shocked fluid where the disturbance has occurred $h_{o,y}$, $T_{o,y}$, and $P_{o,y}$, we can solve for the shock speed S and the shocked fluid properties u_y , T_y , P_y , and ρ_y . These estimates require the use of an accurate equation of state, especially when multiphase or high pressure systems are involved. The unsteady force due to the shock is given by:

$$\boxed{F_u = u_y \rho_y A_p S} \quad (14)$$

In order to facilitate the formulation of a solution, we consider the specific case of an ideal gas where PVT and specific enthalpy h are described using the following simple expressions:

$$\rho = \frac{M_w P}{R_g T} \quad (15)$$

$$c_S = \sqrt{\frac{\gamma R_g T}{M_w}} \quad (16)$$

$$P = \rho e (\gamma - 1) \quad (17)$$

$$h = \frac{P}{\rho} \left[\frac{\gamma}{\gamma - 1} \right] = \frac{R_g T}{M_w} \left[\frac{\gamma}{\gamma - 1} \right] = \frac{c_S^2}{\gamma - 1} \quad (18)$$

where γ is the ideal gas heat capacity ratio of constant pressure to constant volume heat capacities, h is the specific enthalpy, e is the specific internal energy, and R_g is the gas constant. Substitution of the ideal gas forms for ρ and h and rearrangement of the above equations across the shock yields the following expressions:

Mass

$$\rho_y (S - u_y) = \rho_x (S - u_x) \quad (19)$$

Momentum

$$\rho_x (S - u_x)^2 - \rho_y (S - u_y)^2 = (P_y - P_x) \quad (20)$$

Energy

$$h_x - h_y + \frac{1}{2} \left[\frac{P_y - P_x}{\rho_y} \right] \left[\frac{\rho_y}{\rho_x} + 1 \right] = 0 \quad (21)$$

PVT

$$P_y M_{w,y} = \rho_y R_g T_y \quad (22)$$

Boundary Condition

$$h_{o,y} = \frac{P_y}{\rho_y} \left[\frac{\gamma_x}{\gamma_x - 1} \right] + \frac{1}{2} u_y^2 \quad (23)$$

Further reduction of these equations yields working equations that can be solved as a function of P_y/P_x for the shock properties:

$$\frac{\rho_y}{\rho_x} = \left(\frac{\gamma_x + 1}{\gamma_x - 1} \frac{P_y}{P_x} + 1 \right) \left(\frac{\gamma_x + 1}{\gamma_x - 1} + \frac{P_y}{P_x} \right)^{-1} \quad (24)$$

$$\frac{T_y}{T_x} = \frac{P_y \rho_x}{P_x \rho_y} \quad (25)$$

$$S = u_x + c_x \sqrt{\frac{\gamma_x + 1}{2\gamma_x} \frac{P_y}{P_x} + \frac{\gamma_x - 1}{2\gamma_x}} \quad (26)$$

$$u_y = u_x + c_x \left(\frac{P_y}{P_x} - 1 \right) \sqrt{\frac{2}{\gamma_x(\gamma_x - 1)} \left(\frac{\gamma_x + 1}{\gamma_x - 1} \frac{P_y}{P_x} + 1 \right)^{-1}} \quad (27)$$

$$h_y = \frac{P_y}{\rho_y} \left[\frac{\gamma_x}{\gamma_x - 1} \right] + \frac{1}{2} u_y^2 \quad (28)$$

where h_y must be equal to $h_{o,y}$ for the correct solution of P_y/P_x . Note that the entropy change across the shock is not zero:

$$\frac{\Delta s}{R_g} = \frac{\gamma_x}{\gamma_x - 1} \ln \frac{T_y}{T_x} - \ln \frac{P_y}{P_x} \quad (29)$$

where Δs is the entropy change across the shock. These simple equations can be used to estimate the shock properties at low pressures. More complex solutions can be obtained using a detailed equation of state for multiphase systems. These solutions are available in SuperChems Expert.

For the general case involving non-ideal fluids and mixtures, an effective solution method can be used by first guessing the value of ρ_y/ρ_x starting from 1. Once the ratio is specified, the value of u_y is estimated by solving the following equation for u_y :

$$\frac{1}{2} u_y^2 = h_{o,y} - h_{o,x} - \frac{1}{2} \left[\frac{\rho_x}{\rho_y} (S - u_x)^2 - (S - u_y)^2 \right] \left[\frac{\rho_y}{\rho_x} + 1 \right] \quad (30)$$

where S is given by:

$$S = \frac{u_y - \frac{\rho_x}{\rho_y} u_x}{1 - \frac{\rho_x}{\rho_y}} \quad (31)$$

Once u_y is estimated, P_y can be obtained directly from the momentum equation. T_y is then solved for using the energy equation. Knowing T_y and P_y and using a suitable equation of state, ρ_y is estimated. This process is repeated until the estimated value of ρ_y equals the initial estimate.

To obtain the solution to a sudden valve closure (full or partial) using the above equations, set the initial properties of the undisturbed fluid x to the initial values of the flowing fluid causing the disturbance:

$$u_x = -u_{o,y} \quad (32)$$

$$T_x = T_{o,y} \quad (33)$$

$$P_x = P_{o,y} \quad (34)$$

$$h_x = h_{o,y} \quad (35)$$

$$\rho_x = \rho_{o,y} \quad (36)$$

and set the boundary condition to:

$$u_y + u_{y,closed} = 0.0 \quad (37)$$

For a sudden valve closure involving a flowing incompressible fluid, these equations will yield a maximum pressure that is exactly equal to:

$$P_y = P_{o,y} + \rho_{o,y} c_{o,y} (u_{o,y} - u_{y,closed}) \quad (38)$$

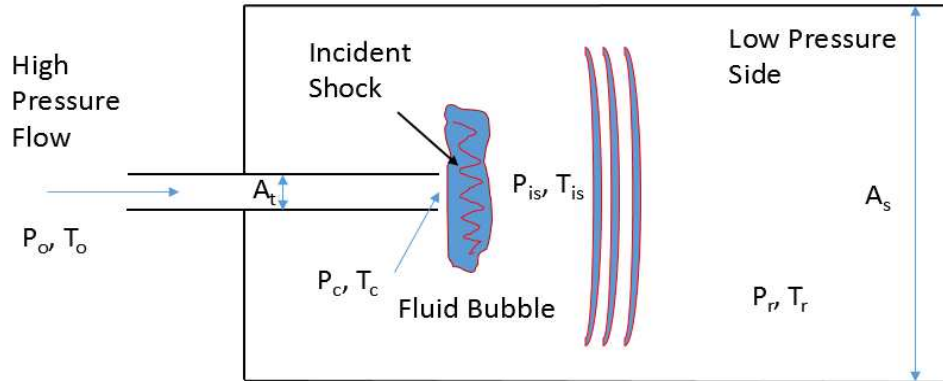
which is a popular equation used to estimate the maximum upstream shock pressure achieved for water hammer problems.

The analysis presented above is most appropriate for compressible single phase vapor/gas flow or compressible two-phase flow. In general, equation of state estimates of liquid speed of sound may not be accurate enough for some liquids such as water. Use of the equations above can overestimate the shock pressure for a high pressure vapor/gas or a high pressure two-phase mixture flow striking a low pressure liquid in some situations, especially where the low pressure fluid side is water. The analysis above works well for situations such as the shock loading that occurs immediately following the fast opening of a rupture disk in a relief line protecting a high pressure process vessel where the high pressure fluid is either gas or two-phase and the low pressure fluid is either gas or two-phase.

8 Surge Pressure Caused by High Pressure Fluid

Note that the initial shock pressure is a short duration pulse that passes through the fluid and tubes, created by the tube rupture. However, because it is not in contact with the walls simultaneously, it is not typically considered to be structurally significant. The initial step pressure of more concern

Figure 5: Simplified representation of events following a tube rupture



is the start of a suddenly increasing but sustained pressure as a result of a pressure surge that passes through the liquid as it starts to move away from the incoming gas.

This initial step surge pressure passes through the heat exchanger and into adjacent piping. It is reflected off any closed segments and partially reflected off diameter reductions, such as entry to the pipes. The duration of these pressures depends on the relative lengths in the heat exchanger shell, attached piping, and distance(s) to any relief device(s) that may be present for pressure protection.

There are many practical applications where we need to consider a high pressure fluid striking a low pressure liquid (see Figure 5). Practical examples include the sudden failure of a tube containing high pressure gas in a shell and tube heat exchanger containing a low pressure liquid on the shell side and the sudden failure of a control valve leading to gas blow through from a high pressure vessel to a low pressure vessel following loss of liquid level and displacement [9].

As the high pressure fluid (liquid, vapor, or two-phase) expands into the low pressure medium (liquid), the local pressure in the low pressure medium can increase to very high values depending on the compressibility of the liquid because the fluid bubble has to overcome the inertia of the liquid. The magnitude of this initial pressure pulse, P_{is} , depends on the upstream pressure, P_c , and the ratio of the effective tube flow area A_t to the characteristic shell liquid flow area, A_s . Essentially, the volume change of the expanding fluid bubble must be matched by the volume change due to the regression of the liquid/fluid interface caused by the passage of the hydraulic pressure wave [2]:

$$\dot{V}_B = A_s \Delta u_{is} = A_s \frac{\Delta P_{is}}{\rho l c_{lS}} = A_s \frac{P_{is} - P_r}{\rho l c_{lS}} \quad (39)$$

where \dot{V}_B is the fluid bubble volumetric rate of change due to compression, Δu_{is} is the imposed initial liquid velocity, $\Delta P_{is} = \rho_l \Delta u_{is} c_{lS}$ is the initial fluid impact induced step increase in pressure (commonly known as water hammer) from the Joukowsky equation, $P_{is} = P_r + \Delta P_{is}$ is the fluid induced initial pressure, P_r is the low pressure medium operating pressure, ρ_l is the low pressure medium liquid density, and c_{lS} is the isentropic speed of sound [7] in the liquid adjusted for the presence of dissolved gas, the shell material of construction elasticity, and structural support conditions.

For bulk fluid flow, if the fluid velocity is disturbed by Δu the corresponding pressure change ΔP can be approximated by differentiating the the change in dynamic pressure $\frac{1}{2}\rho u^2$:

$$\Delta P = \Delta \left(\frac{\rho u^2}{2} \right) = \frac{\rho}{2} (\Delta u)^2 \quad (40)$$

If ΔP acts on a flow area A to accelerate a fluid region at density ρ and length L , then a response time can be calculated from Newton's law:

$$A\Delta P = \rho A \frac{L}{\Delta t} \Delta u = A \frac{\rho}{2} (\Delta u)^2 \quad (41)$$

leading to:

$$\Delta t = 2 \frac{L}{\Delta u} \quad (42)$$

8.1 Gas Flow Striking a Liquid

In the case where the upstream fluid is a high pressure gas, the volumetric flow rate through the tube rupture of the expanding high pressure gas at the choke pressure can be given by:

$$\dot{V}_c = C_d A_t c_{gS} \quad (43)$$

where \dot{V}_c is the volumetric flow rate of the gas, A_t is the effective flow are of the tube normally taken to be twice the flow area of one tube, and C_d is the discharge coefficient for the tube effective flow area, and c_{gS} is the gas isentropic speed of sound. If we assume ideal gas behavior for the flowing high pressure gas, then:

$$c_{gS} = \sqrt{\frac{\gamma R_g T_c}{M_w}} \quad (44)$$

where $T_c = \left(\frac{2}{\gamma+1} \right) T_o$ is the choke temperature at the choke pressure $P_c = P_o \left[\left(\frac{2}{\gamma+1} \right)^{\gamma/(\gamma-1)} \right]$, R_g is the universal gas constant, and M_w is the gas molecular weight. The volumetric flow rate through the tube rupture of the expanding high pressure gas at the choke pressure becomes:

$$\dot{V}_c = C_d A_t \sqrt{\frac{\gamma R_g T_c}{M_w}} \quad (45)$$

If we assume the expansion of the high pressure gas into the low pressure medium follows an isentropic thermodynamic path, then:

$$P_c \dot{V}_c^{\nu_S} = P_{is} \dot{V}_B^{\nu_S} \quad (46)$$

where ν_S is the isentropic gas coefficient¹ which is equal to γ for an ideal gas. As a result, and for an ideal gas:

$$P_{is} (P_{is} - P_r)^\gamma = \underbrace{P_o \left(\frac{2}{\gamma + 1} \right)^{\gamma/(\gamma-1)}}_{P_c} (c_{gS} \rho_l c_{lS})^\gamma \left(\frac{C_d A_t}{A_s} \right)^\gamma \quad (47)$$

or

$$P_{is} (P_{is} - P_r)^\gamma = P_c (c_{gS} \rho_l c_{lS})^\gamma \left(\frac{C_d A_t}{A_s} \right)^\gamma \quad (48)$$

If we assume that $P_r \ll P_{is}$ then:

$$P_{is} \simeq P_c^{\frac{1}{\gamma+1}} (c_{gS} \rho_l c_{lS})^{\frac{\gamma}{\gamma+1}} \left(\frac{C_d A_t}{A_s} \right)^{\frac{\gamma}{\gamma+1}} \quad (49)$$

Equation 49 shows that the value of P_{is} will increase with a decreasing value of A_s . P_{is} is highest with a single tube that has the same flow area as the shell. Equation 49 also shows that higher values of P_{is} are achieved with higher fluid speed of sound and liquid density, such as high pressure hydrogen striking water. For example, at upstream conditions of 100 barg and 100 C, hydrogen flow will choke isentropically at 51.5 barg and 35 C with a speed of sound of 1372 m/s. The gas isentropic expansion coefficient at the choke point is 1.45. As a result:

$$\begin{aligned} P_{is} &\simeq (52.5 \times 100,000)^{0.408} (1372 \times 1000 \times 1427)^{0.59} \left(\frac{C_d A_t}{A_s} \right)^{0.59} \\ &= 551.85 \times 303,493 \times \left(\frac{C_d A_t}{A_s} \right)^{0.59} \\ &= 1,674.84 \text{ bara} \times \left(\frac{C_d A_t}{A_s} \right)^{0.59} \end{aligned}$$

If the effective tube flow area is 1 % of A_s then P_{is} would be equal to 110.65 bara. Using smaller tube flow areas can reduce the value of P_{is} . It may be practical in some cases to select a tube flow area to shell effective flow area such that the maximum value of P_{is} is well within the hydrotest pressure limit which may eliminate the need for large pressure relief systems.

Reference [2] provides practical guidance for the calculation of A_s . A_s is the effective cross-sectional area of the liquid in the shell that is in the path of the expanding fluid bubble which is dependent on the heat exchanger geometry. For a shell and tube heat exchanger with a longitudinal baffle configuration, A_s is simply the cross sectional area of the shell in one pass minus the total cross sectional area of all the tubes. For a transverse baffle configuration, the pressure wave has to travel around each of the baffles with multiple changes in direction. A_s can be estimated by establishing the total effective volume of the liquid in the shell pass (total shell pass volume minus total volume of the tubes) and dividing the total effective liquid volume by the actual distance the

¹Note: $\nu_S = -\frac{V}{P} \left(\frac{\partial P}{\partial V} \right)_S = \frac{1}{\kappa_T P} \frac{C_p}{C_v} = \frac{\rho}{P} c_S^2 = \frac{1}{\kappa_S P} = \gamma$ for an ideal gas

pressure wave travels from the tube rupture around each baffle, L_e . If the break occurs at the top of the tubesheet, the estimated effective flow path length of the gas equals to:

$$L_e = (N + 1)D + L \quad (50)$$

where N is the number of transverse baffles, D is the inside diameter of the shell, and L is the length of the shell.

8.2 Liquid Flow Striking a Liquid

We can apply the same method above for the calculation of P_{is} if the upstream high pressure fluid is a liquid also. In this case,

$$\dot{V}_o = C_d A_t u_l = C_d A_t \sqrt{\frac{2}{\rho_o} (P_o - P_r)} \quad (51)$$

and P_{is} can be calculated like before by equating \dot{V}_o to \dot{V}_B :

$$\dot{V}_B = A_s \Delta u_{is} = A_s \frac{\Delta P_{is}}{\rho_l c_{lS}} = A_s \frac{P_{is} - P_r}{\rho_l c_{lS}} = \dot{V}_o = C_d A_t u_l \quad (52)$$

As a result:

$$P_{is} = P_r + \rho_l u_l c_{lS} \frac{C_d A_t}{A_s} \quad (53)$$

Equation 53 recovers the well known Joukowsky pressure surge equation in Equation 38 if $\frac{C_d A_t}{A_s} = 1$.

8.3 Two-Phase and/or Non-Ideal Fluid Flow Striking a Liquid

If the upstream high pressure fluid is a two-phase mixture or a non-ideal fluid, then the calculation of P_{is} requires trial and error:

1. Calculate T_c , P_c , \dot{V}_c and the vapor quality using using direct VdP integration over an isentropic flow path from P_o to the pressure that will maximize flow, P_c . A two-phase pipe flow calculation can be performed for the long portion of the tube.
2. Guess P_{is}
3. Calculate $\dot{V}_{B1} = \frac{A_s(P_{is}-P_r)}{\rho_l c_{lS}}$
4. Isentropically compress the fluid from T_c and P_c to P_{is} and calculate the associated temperature T_{is} , vapor quality, density, and volumetric flow rate, \dot{V}_{B2}
5. Calculate $F = \dot{V}_{B1} - \dot{V}_{B2}$. Iterate on P_{is} until $F = 0$.

This detailed numerical method is used by SuperChems Expert to calculate P_{is} for single and multi-phase flow. It is particularly useful because it can handle retrograde and phase change and can deal with supercritical fluid flow as well.

9 Reaction Forces

The rapid opening of a relief device or the sudden rupture of a heat exchanger tube can result in large and rapid changes in flow rate which can subject the relief piping systems to transient forces, transient impulses, and quasi-steady state forces. Depending on the piping layout, significant moments may be generated in the relief piping and associated equipment. The piping overall transient force can be represented in one dimension as a function of time:

$$F(t) = \underbrace{u_c \dot{M} + (P_c - P_a) A_c}_{\text{Thrust load, } F_s} + \underbrace{\frac{\partial}{\partial t} \int \rho u A dx}_{\text{Wave load, } F_u} = F_s + F_u \quad (54)$$

where F_s is the steady state reaction force (steady state thrust load) applied to the piping supports, u_c is the velocity just inside the exit plane of the pipe, \dot{M} is the mass flow rate, P_c is the absolute pressure just inside the exit plane of the pipe, A_c is the exit area of the pipe, and P_a is the ambient absolute pressure. The thrust load includes the momentum flux of the discharging fluid and the differential pressure at the exit. F_s is often considered for piping support design as the reaction force produced when a fluid is discharged from the end of a pipe to the atmosphere. Because closed piping systems under steady flow do not exert a reaction force onto their supports, this reaction force is the only steady state reaction force that is applied to the piping supports:

$$\boxed{F_s = u_c \dot{M} + P_c A_c - P_a A_c} \quad (55)$$

F_u is the unsteady reaction force (wave load) applied to the piping supports and x is distance down the pipe segment. The wave load is the unsteady reaction force caused by the rate of fluid momentum change. The wave load approaches zero at steady state. The magnitude of F_u is proportional to the rate of change in the relief mass flow within the piping. Depending on the relief scenario and pipe segment length, the duration may be of the order of a few milliseconds to several seconds. The transient force is frequently neglected for gas phase relief but can be significant for liquid or two-phase relief:

$$F_u = \frac{\partial}{\partial t} \int \rho u A dx \quad (56)$$

This transient reaction force can also be approximated by:

$$F_u = \frac{d}{dt} (\rho u A L) = \frac{d}{dt} (\dot{M} L) = L \frac{\dot{M}_2 - \dot{M}_1}{t_2 - t_1} \quad (57)$$

Where \dot{M} is the mass flow rate, t is the arrival time, subscript 1 refers to the pipe inlet plane and subscript 2 refers to the pipe exit plane. Transient loads tend to be applied for short durations, tens of milliseconds to several seconds. In many cases the initial flow \dot{M}_1 is zero and t_1 is also equal to zero. It is recommended that the mass flow rate \dot{M} be calculated without the influence of piping resistance (nozzle estimate) and at the maximum allowable pressure accumulation in the vessel. As a result,

$$\boxed{F_u = L \frac{\dot{M}}{\Delta t} = \frac{\dot{M}^2}{\rho A_c}} \quad (58)$$

When analyzing structures for short duration structural loads, it may be useful to include the impulse. The impulse is the product of the load application times the duration:

$$I = \int_{t_1}^{t_2} F_u dt \quad (59)$$

F_u typically decays over time after the sudden opening of a relief device or flow element. If we assume the decay occurs linearly (triangular shape), then:

$$I = \int_{t_1}^{t_2} F_u dt = \frac{F_u \Delta t}{2} \quad (60)$$

or

$$\boxed{\Delta t = 2 \frac{I}{F_u}} \quad (61)$$

Using the approximated expression of F_u above results in a simple equation for impulse:

$$I = L (\dot{M}_2 - \dot{M}_1) \quad (62)$$

If the flow changes between two steady state conditions, the net impulse that is applied to the piping supports is equal to the length of the pipe segment times the difference in the steady state flows. In many cases the initial flow \dot{M}_1 is zero and the impulse is equal to the segment length times the final mass flow rate. It is recommended that the mass flow rate \dot{M}_2 be calculated without the influence of piping resistance (nozzle estimate):

$$\boxed{I = L \dot{M}} \quad (63)$$

In addition to the overall transient force $F(t) = F_s + F_u$, relief piping can also experience an increase in the tension force within the piping, F_{PT} (see [10]). Usually, the tension force used in designing flanges and other joints is based upon the piping design pressure. The selected design pressure will typically have enough margin where any increased tension due to flow does not impact the design. High fluid velocities such as those encountered in relief systems applications can result in higher piping tension forces than those that are typically obtained from the operating pressure. The piping tension force can be calculated from:

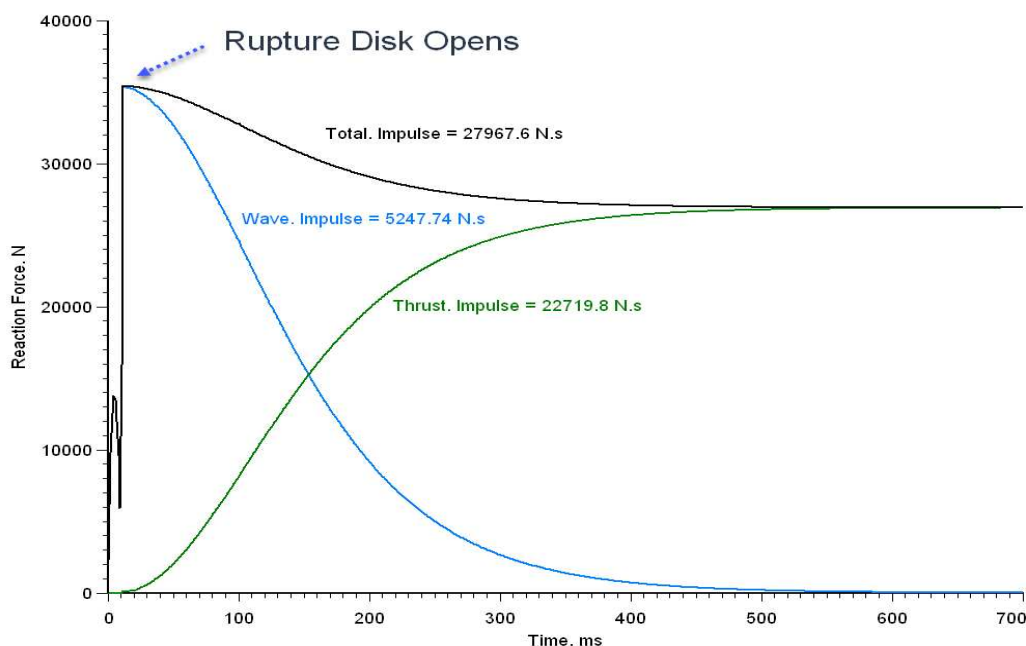
$$\boxed{P_{PT} = \frac{F_{PT}}{A_p} = P_i + \frac{F_u}{A_p} - P_a} \quad (64)$$

where F_{PT} is the pipe tension force, P_i is the initial local pipe absolute pressure which is typically ambient pressure, P_a is the ambient absolute pressure and P_{PT} is the minimum design pressure for tension loads which is equal to F_{PT}/A_p or:

$$\boxed{\frac{P_{PT}}{P_i} = 1 - \frac{P_a}{P_i} + \frac{F_u}{P_i A_p}} \quad (65)$$

where F_u is the transient reaction force experienced upon opening of the pressure relief device defined earlier in equation 58. Usually other piping design considerations lead to higher pipe design pressure values than P_{PT} . The mass flow rate value used in equation 58 should be calculated at the maximum allowable pressure accumulation in the vessel.

Figure 6: Reaction Force Components and Associated Impulse Values as Calculated by SuperChems Expert v8.40



9.1 Example

We consider a 6 inch NPS (0.0186 m² flow area), 9 m long inlet relief line that contains water and is at an initial pressure of 1 bara (100,000 Pa) and room temperature. A 6 inch rupture disk with a Kr value of 1.5 and an opening time of 2 ms separates the inlet line from the discharge point. The stagnation pressure of the source increases from 1 bara to 20 bara over 10 ms. The discharge backpressure is constant at 1 bara. An equivalent discharge coefficient $C_d \simeq 0.58$ is calculated to account for the rupture disk Kr value and the inlet line entrance effects and frictional pressure loss.

Figure 6 shows the calculated reaction force components as a function of time using the detailed 1D dynamics model of SuperChems Expert. Impulse loads are also reported for a total duration of 1 second. The dynamics show that the mass flow rate reaches 583 kg/s at steady state (> 300 ms). We note from Figure 6 that the wave component decreases and tends to zero at steady state while the thrust component increases and remains constant at steady state.

It is very interesting to note that because the piping is short the estimate of wave impulse value using the simple form in equation 63 yields almost exactly the same answer as the detailed dynamics:

$$I = \dot{M}L = 583 \times 9 = 5,247 N.s \quad (66)$$

We can also approximate the duration of the wave loading by calculating the maximum value of

F_u :

$$F_u = \frac{\dot{M}^2}{\rho A_c} = \frac{583^2}{1000 \times 0.58 \times 0.0186} = 31,506 \text{ N} \quad (67)$$

The duration of wave for a triangular shape equals:

$$\Delta t = 2 \frac{I}{F_u} = 2 \frac{5247}{31,506} = 0.333 \text{ s or } 333 \text{ ms} \quad (68)$$

The value of 333 ms is very close to the duration of the wave load as shown in Figure 6. The minimum design pressure for tension loads P_{PT} for the downstream discharge piping (6 inch NPS) is given by:

$$\frac{P_{PT}}{P_i} = 1 - \frac{P_a}{P_i} + \frac{F_u}{P_i A_p} = 1 - 1 + \frac{31,506}{100,000 \times 0.0186} = 16.93 \quad (69)$$

9.2 The Use of Dynamic Load Factors

When a load is quickly applied to a structure, the structure vibrates similar to a mass being supported by a spring. This dynamic response results in instantaneous loads within the structure that are greater than the applied load. Because structures are usually analyzed using static models instead of using dynamic structural models, a dynamic load factor is typically used to relate the equivalent load to the applied load [10].

$$F_{eq} = DLF \times F_s \quad (70)$$

where F_{eq} is the equivalent static load and DLF is the dynamic load factor. For loads that are applied quickly and that are of long duration the dynamic load factor varies between 1 and 2. A value of 2 is recommended. Please refer to the CCPS Guideline [10] for more specific information about recommended values for the dynamic load factors for pressure relief valves and rupture disks in gas, liquid, and two-phase service.

A load is considered to be applied quickly if the rate of application is short compared to the natural frequency of the structure. The application rate is considered to be slow if the time is long compared to the structural natural frequency. The same principles hold for the load duration. If the duration of the load is short, then the dynamic load factor can vary from 0 to 2. The use of the dynamic load factor is only appropriate when a static analysis is performed on the structure. If a dynamic structural analysis is to be done, then the dynamic load factor should not be used because the analysis will include the effect of dynamic loading. When a time history pipe stress model is used, the DLF is captured by the participating elements and inertial response.

When using a dynamic load factor, the analysis is only valid for the single application of a load to a structure. If a load is applied repeatedly to a structure, then resonance may occur. A term from vibration theory that is used to relate the applied load to the equivalent load when resonance may occur is the magnification factor. Depending on the applied frequency, structural natural frequency, duration, and dampening, the magnification factor may vary between 0 and 10 or more.

10 Structural Loads Following Tube Failure

Transient reaction forces on the shell and relief systems piping caused by the initial acceleration of the liquid slug should be considered. This is a form of the Joukowski pressure which can be used to determine a pressure surge as shown earlier. Piping and piping components upstream and downstream of the relief device are exposed to reaction forces: (a) forces due to the surge pressure upstream of the relief device, and (b) forces due to the movement of the liquid slug entering the downstream piping once the relief device opens. All forces should consider the Dynamic Load Factor.

The duration of the transient reaction force on the relief systems piping caused by the acceleration of the initial liquid slug will depend on the relative locations of elbows and fittings and the shape of the pressure wave, i.e. whether it includes any reflections or not. Once the slug enters the piping downstream of the relief device, the duration of a reaction force is a function of the slug velocity.

We will consider structural loads for three distinct phases following a sudden tube rupture:

- a) Forces applied to the shell due to the initial acceleration of the liquid in the shell (upstream of the relief device),
- b) Transient reaction forces applied to the shell side relief piping during initial liquid flow (downstream of the relief device), and
- c) Quasi-steady reaction forces applied to the shell side relief piping during established initial liquid flow, followed by two-phase flow, and finally all gas flow.

10.1 (a) Shell Side Liquid Acceleration Forces

Immediately after the tube failure, the shell experiences a short duration transient force associated with the initial acceleration of the liquid in the shell. This force is caused by the pressure discontinuity where the passing of the pressure wavefront produces a force:

$$F_u = \rho_l \Delta u_{is} A_s c_{l_s} = \Delta P_{is} A_s \quad (71)$$

If the shell length is L_s and time required for the tube to completely rupture is t_{open} , the initial pressure wave will be completely contained within the shell for a period of:

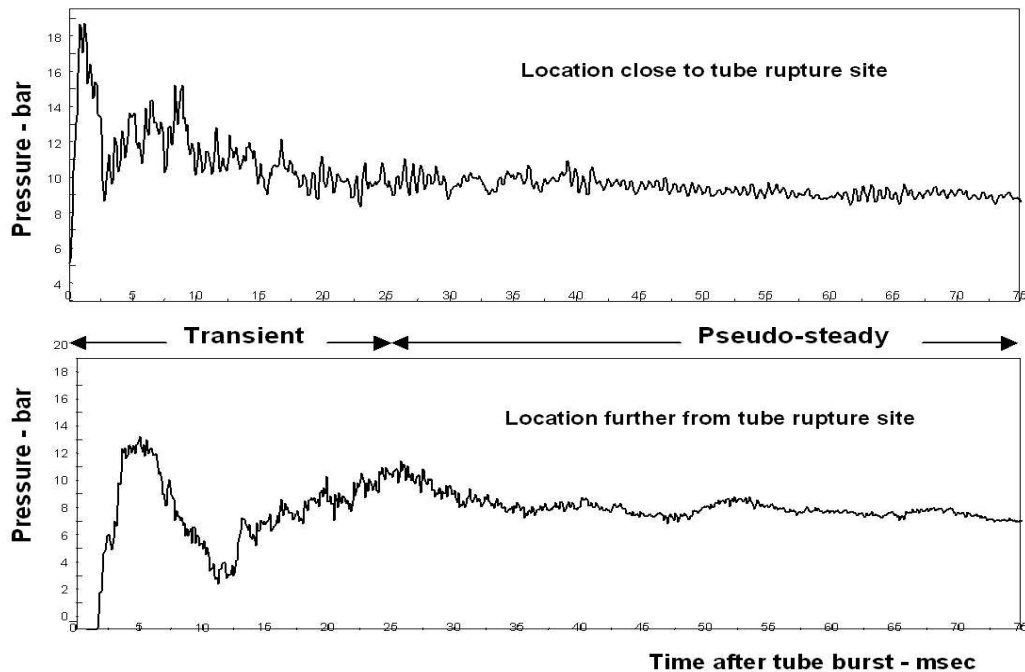
$$t_u = \frac{L_s}{c_{l_s}} - t_{open} \quad (72)$$

The trailing edge of the pressure wave in the shell will be at $t_{open} \times c_{l_s}$. It is not always possible to locate a relief device next to where the tube rupture will happen and as a result the initial pressure can be reflected at closed ends and the reflection adds another ΔP_{is} to the load:

$$F_u = 2\rho_l \Delta u_{is} A_s c_{l_s} = 2\Delta P_{is} A_s \quad (73)$$

The Institute of Petroleum [1, 11] conducted several tests to better understand the impact of short duration high amplitude structural loads exhibited by the shell (liquid) following instantaneous

Figure 7: Typical shell side pressure transients following a sudden tube rupture [1, 11]



high pressure (gas) tube ruptures. Figure 7 illustrates the pressure transient experienced on the shell side following a sudden tube rupture at a location close to the tube rupture point and a location that further from the tube rupture point. Note the time shift associated with the transit time of the pressure wave from near the failure point to the location that is further from it.

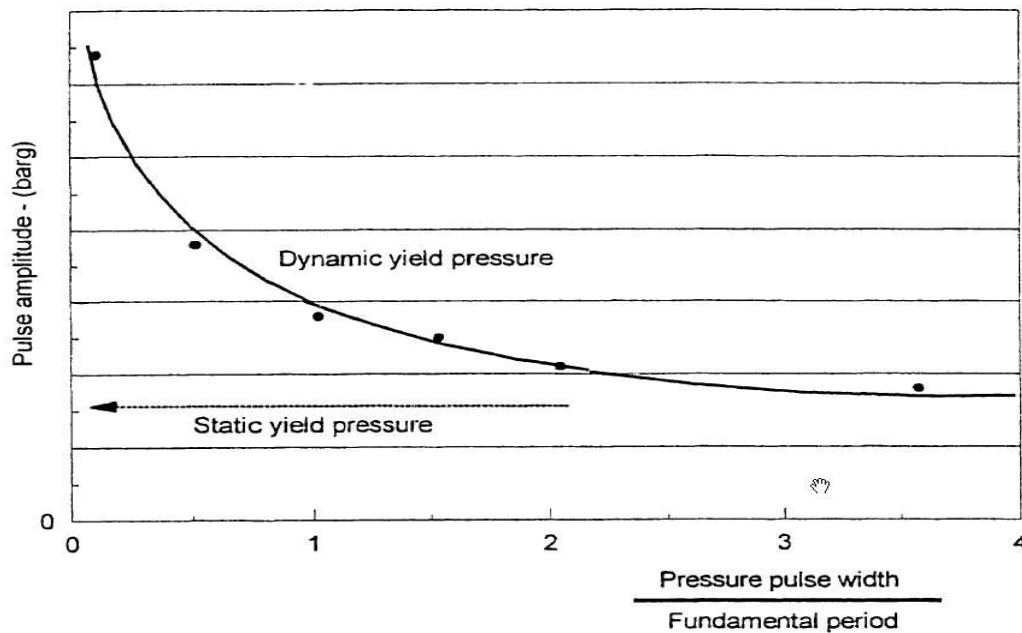
The heat exchanger used by the Institute of Petroleum was a 3.75 m long steel shell with an internal diameter of 0.74 m containing a standard tube bundle with internal tube diameters of 15 mm each. Although the measured peak pressures are high compared to the pressure rating of the shell, their durations were short on the order of 5 ms. These short durations are typically less than the natural frequency of the shell, in this case 9.8 ms. Under such short duration dynamic loads, the shell can possibly tolerate more than the static yield limit as shown in Figure 8.

These measurements highlight the importance of the relief device opening times and relief device location relative to the failure point. The magnitude and duration of the pressure transients can be reduced with the use of multiple and optimally located relief devices with fast opening times.

10.1.1 Initially Liquid Full Relief Discharge Piping

It is undesirable to have relief discharge piping that is initially liquid filled because the sudden opening of a relief device or the failure of a tube under high pressure can create large transient reaction forces on the piping. If the opening of the relief device or tube rupture is short compared to the time required for the pressure wave to travel the pipe segment, then the maximum applied reaction force for a straight pipe segment can be approximated as the burst pressure times the flow area of the pipe segment. In the case of a tube rupture, the maximum applied reaction force for a

Figure 8: Dynamic shell failure limits as a function of pressure pulse durations [1, 11]



straight pipe segment is given by Equation 71. If the opening of the relief device or tube rupture is long compared to the time required for the pressure wave to travel the pipe segment, then the applied reaction force to segment i is given by:

$$F_{u,i} = \Delta P_{is} A_i \frac{L_i}{L_T} \quad (74)$$

where $F_{u,i}$ is the reaction force applied to segment i , A_i is the pipe segment flow area, L_i is the length of segment i , and L_T is the total length of the relief discharge pipe. The reaction force can be significantly higher if resonance occurs between the structural natural frequency and the acoustic natural frequency of the liquid filled line.

The pressure wave will reflect back and forth in the line until steady state flow is achieved. The impulse can be calculated more easily using the steady state mass flow rate rather than the actual dynamic reaction force and often serves as a better design criterion. Frequently, the duration of the dynamic reaction force is so short that the structural support for the piping does not have enough time to respond to the loading. The impulse considers both the load and duration of the load. It is the integral of the applied reaction force over time. The impulse for pipe segment i is calculated as:

$$I_i = L_i \dot{M} \quad (75)$$

where \dot{M} is the steady state flow rate.

10.2 (b) Relief Piping Transient Liquid Reaction Forces

The shell side can either be protected with a fast acting rupture disk or a PRV. It has been shown through actual field tests that the opening time for PRVs can be as low as 5 to 7 milliseconds. This response time is enhanced by the high pressure water hammer wave as it passes the device. Initially, the relief discharge line is empty of liquid and full of air or methane or nitrogen. The transient reaction force is primarily due to the liquid filling the discharge pipe and the duration of this transient load is approximately equal to the time it takes the liquid to fill the discharge pipe. These transient reaction forces are particularly important for liquid and two phase discharges. Since the relief discharge piping is initially empty, the liquid or two-phase mass flow rate should be calculated assuming no piping resistance to flow.

Due to the uncertainty of the liquid-gas interface in the relief discharge piping, a dynamic load factor of 2 should be applied to the reaction forces calculated below for liquid flow. The dynamic load factor should not be applied if a dynamic structural analysis is being performed. The factor of 2 should only be used if a static analysis is being performed with the transient loads calculated below.

10.2.1 Rupture Disk

The transient reaction force for a rupture disk is proportional to the pressure difference of the rupture disk opening pressure and the relief piping backpressure:

$$F_u = \frac{\dot{M}^2}{\rho_l A_p} = \frac{2\Delta P A_p}{1 + K_{ent} + K_r} = \frac{2(P_{open} - P_a) A_p}{1 + K_{ent} + K_r} = 2(P_{open} - P_a) A_p C_d^2 \quad (76)$$

where A_p is the flow area of the pipe, \dot{M} is the liquid flow rate through the rupture disk, K_{ent} is the number of velocity heads lost in the inlet piping between the shell and the rupture disk, K_r is the loss through the rupture disk assembly, P_{open} is the maximum pressure at which the rupture disk is expected to open which is not necessarily equal to the set point depending on the manufacturing range of the rupture disk, and P_a is the backpressure. Conservative estimates can be obtained by assuming K_{ent} and K_r are zero.

A relief discharge piping segment of length L_i is subjected to an impulse load equal to:

$$I = \dot{M} L_i = A_p L_i \sqrt{\frac{2\rho_l (P_{open} - P_a)}{1 + K_{ent} + K_r}} = C_d A_p L_i \sqrt{2\rho_l (P_{open} - P_a)} \quad (77)$$

The duration of this transient reaction force is calculated by:

$$t_u = 2 \frac{I}{F_u} = 2 \frac{\dot{M} L_i}{F_u} \quad (78)$$

10.2.2 Pressure Relief Valve

Transient reaction forces from liquid and two-phase flow from a PRV are calculated similarly to those from a rupture disk. However, in the case of a PRV the transient force may be significantly

reduced if the time required to reach full flow from the PRV (from 0 % to 10 % overpressure for example) is longer than the time it takes to fill the pipe.

$$F_u = \frac{\dot{M}^2}{\rho_l A_p} \quad (79)$$

$$I = \dot{M} L_i \quad (80)$$

$$t_u = 2 \frac{I}{F_u} = 2 \frac{\dot{M} L_i}{F_u} \quad (81)$$

10.3 (c) Relief Piping Steady State Liquid Reaction Forces

A steady state reaction force is exerted on the piping when liquid is discharged to the atmosphere. The reaction force is equivalent to liquid mass flow times liquid velocity because liquid flows are almost always subsonic:

$$F_s = u_l \dot{M} + \underbrace{(P_c - P_a) A_p}_0 = u_l \dot{M} \quad (82)$$

A dynamic load factor of 2 is also applied to this reaction force:

$$F_{eq} = DLF \times F_s = 2F_s \quad (83)$$

10.4 Ethylene STHE - Shell Side Liquid Acceleration Forces

We continue the ethylene STHE evaluation by calculating the initial incident pressure upon tube failure so that we can assess if the shell is likely to survive this initial pressure pulse. First, we derate the shell side flow area by 10 % to add a reasonable safety margin to the incident pressure estimates as recommended by the Energy Institute, leading to a flow area on the shell side of 320 in².

The calculated reflected peak incident pressure value is 420 psig which is approximately equal to the hydrostatic test pressure of 410 psig for the shell adjusted for maximum operating temperature. The reflected pressure value has to be used because it is difficult to know the location of the tube rupture relative to the location of the pressure relief device. We also note that the duration of this initial pressure pulse will be close to 9 ms because the shell diameter to thickness ratio is approximately 100 leading to a 30 % reduction in the pipe/fluid speed of sound for the shell side. The associated force for the reflected pressure associated with the liquid displacement in the shell is very large at 442 kN (99.23 kips). It would also be useful to establish the natural frequency of the shell as well as the ratio of the duration of the calculated reflected pressure pulse at 8.9 ms to that as shown in Figure 8 for typical dynamic shell failure limits. If the ratio is less than 1, the shell can tolerate a higher dynamic short duration pressure pulse.

The incident pressure would be higher if the fluid on the tube side has a lower molecular weight and/or if the initial gas temperature is higher. For example, if the fluid in the tube was hydrogen

Figure 9: SuperChems Expert calculated initial liquid displacement incident pressure pulse on the shell side

Status	Normal return		
Solver	Use Expanding Fluid Method		
** INITIAL HIGH PRESSURE CONDITIONS			
Stream	TUBE - COMBINED FLOW		
Vapor mole fraction. %	79.938		
Pressure. psig	680.000		
Temperature. F	44.705		
Density. kg/m3	155.244		
Flow velocity. m/s	253.249		
Speed of sound. m/s	253.249		
Speed of sound piping correction factor	1.00		
** INITIAL LOW PRESSURE CONDITIONS			
Stream	SHELL SIDE		
Vapor mole fraction. %	0.000		
Pressure. psig	110.000		
Temperature. F	80.000		
Density. kg/m3	994.089		
Flow velocity. m/s	0.000		
Speed of sound. m/s	1028.746		
Speed of sound piping correction factor	0.69		
** FINAL SHOCKED FLUID CONDITIONS			
	ACTUAL	/LOW P	/HIGH P
Reflected shock pressure. psig	420.106	3.487	0.626
Shock pressure. psig	265.053	2.243	0.403
Shock temperature. F	-22.262	0.811	0.867
Shock density. kg/m3	52.246	0.053	0.337
Shock velocity. m/s	214.535	0.209	0.929
Shocked fluid velocity. m/s	1.045	0.001	0.005
** SHOCK LOADS			
	ACTUAL	REFLECTED	DURATION. ms
Upstream shock load. kN	0.0	0.0	42.15
Downstream shock load. kN	220.7	441.4	8.89

Table 1: Impact of gas molecular weight on shell side liquid displacement loads. $P_o = 2500$ psig, $T_o = 100$ F

	Ethylene	Methane	Hydrogen
Molecular Weight	28	16	2
P_{is} , reflected, psig	420	530	1016
$F_{u,r}$, reflected, kN	442	597	1290
Δu_{is} , m/s	1.05	1.41	3.05

at 2500 psig, and 100 F, the peak incident pressures would increase from 420 psig to 1016 psig as shown in Table 1. As a result, worst case liquid displacement conditions should be expected to occur with high pressure hydrogen at elevated temperatures striking low pressure water.

11 Relief Systems Design and Evaluation

In order to conduct a proper evaluation of the quasi-dynamic behavior for the shell and the adequacy of the existing relief system, we need to consider the following cases:

- A All liquid flow from the existing rupture disk without any discharge piping at the maximum opening pressure of the rupture disk, 5 % in this case. Use 10 % if this value is unknown or uncertain. This design case will be used to establish the initial dynamic reaction force the relief piping will be subjected to when the rupture disk first opens. This analysis can be performed using simple Bernoulli flow if detailed piping flow models are not available. The rupture disk resistance to flow, K_R , should be selected for the fluid phase that initially bursts the rupture disk (liquid in this case) even if during the transient (after bursting) the fluid phase changes to two-phase and then vapor. The flow geometry of the bursted disk causing the resistance to flow is different when opened by liquid from when it is opened by vapor or gas.
- B Transient two-phase flow from the shell to establish the maximum transient pressure level in the shell and the associated quasi-steady state reaction forces that the relief piping will be subjected to. In general, this simulation is the only one needed since the initial flow is almost always 100 % liquid as the incoming high pressure gas pushes the liquid out of the shell through the relief piping.
- C If the pressure in the vessel exceeds a tolerable value, two-phase flow should be used to establish a relief device size such that the maximum pressure reached during quasi-dynamic flow is tolerable. The initial dynamic reaction forces for all liquid flow should be re-computed at this new size and so should the steady state reaction forces.

11.1 A - Relief Piping Transient Reaction Forces from Initial Liquid Flow

After the shell is exposed to the short duration liquid acceleration forces and pressure increases sufficiently to cause the opening of the relief device, the relief piping will be subjected to transient reaction forces. These forces are primarily caused by the discharge piping being filled as the liquid makes its way to the end of the discharge piping. One can use the simple equations provided earlier for either a rupture disk or pressure relief valve, or simply remove the discharge line from the actual relief line and estimate the peak flow at the maximum opening pressure of the relief device, 5 or 10 % for a rupture disk, and 10 % for a PRV.

If we do that for all liquid flow for the ethylene STHE example, we calculate a maximum liquid flow rate of 83.5 kg/s at a stagnation pressure of 268 psig. The discharge piping consists of two segments, a 10 ft, 4 inch NPS (12.730 in² flow area) vertical segment and a 60 ft, 6 inch NPS (28.890 in² flow area) horizontal segment. The transient liquid force applied to each segment is calculated below.

The calculated values for I and F_u below should be multiplied by the DLF of 2 if a static analysis is being performed. The use of the dynamic load factor is only appropriate when a static analysis is performed on the structure. If a dynamic structural analysis is to be done, then the dynamic load factor should not be used because the analysis will include the effect of dynamic loading.

11.1.1 10 ft Segment

$$F_u = \frac{\dot{M}^2}{\rho_l A_p} = \frac{83.5^2}{1000 \times 12.73 \times 0.0254^2} = 849 \text{ N}$$

$$I = \dot{M}L = 83.5 \times 10 \times 0.3048 = 254.5 \text{ N.s}$$

$$t_u = 2 \frac{I}{F_u} = 2 \frac{254.5}{849} = 0.6 \text{ s}$$

11.1.2 60 ft segment

$$F_u = \frac{\dot{M}^2}{\rho_l A_p} = \frac{83.5^2}{1000 \times 28.890 \times 0.0254^2} = 374 \text{ N}$$

$$I = \dot{M}L = 83.5 \times 60 \times 0.3048 = 1527 \text{ N.s}$$

$$t_u = 2 \frac{I}{F_u} = 2 \frac{1527}{374} = 8.16 \text{ s}$$

11.2 B - Quasi-Dynamic Two-Phase Flow

An important part of the evaluation deals with the time dependent increase in pressure in the vessel as high pressure fluid is expanding into the shell and causing relief. Initially, all liquid

Figure 10: SuperChems Expert verification of shell design rating

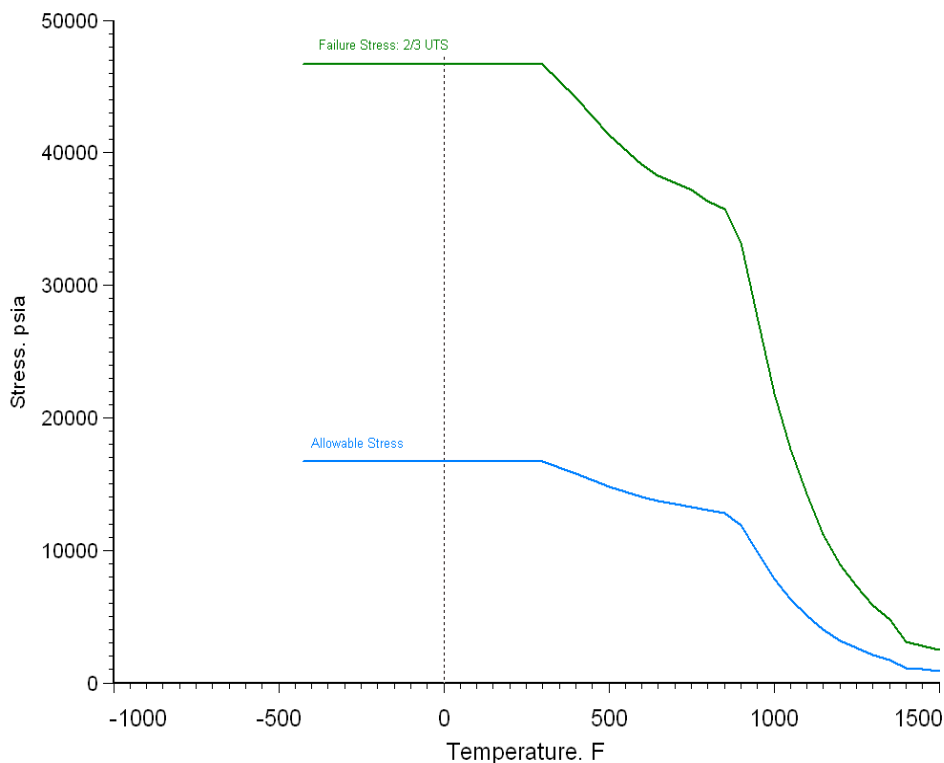
Verify Vessel Design Ratings							
	A	B	C	D	E	F	G
1	Vessel Name	HEAT EXCHANGER					
2	Vessel Type	Vertical Cylindrical; User defined heads					
3	Vessel Top Head Type	Flat					
4	Vessel Bottom Head Type	Flat					
5							
6	** MATERIAL OF CONSTRUCTION SPECIFICATIONS. OBTAIN THIS INFORMATION FROM ASME TABLES						
7	Actual Material of Construction Description	STEEL					
8	Databank material of construction used for thermal	STEEL	STEEL				
9							
10	Specification	A 312					
11	P-No, G-No, or S-No	P-8					
12	Product Form	Seamless Pipe					
13	Grade	TP304L					
14							
15	Note 1	Enter note 1 here					
16	Note 2	Get allowable stress data from ASME tables. this data is for seamless pipe and is used as					
17							
18	Minimum Temperature. F	-425.00					
19	Minimum yield strength. psia	25000.00					
20	Minimum tensile strength. psia	70000.00					
21							
22	Allowable Stress Basis	ASME					
23	Allowable Stress Temperature. F	-425.00	100.00	200.00	300.00	400.00	500.00
24	Allowable Stress. psia	16700.00	16700.00	16700.00	16700.00	15800.00	14800.00
25							
26	Failure Stress Basis	2/3 UTS					
27	Failure Stress Temperature. F	-425.00	100.00	200.00	300.00	400.00	500.00
28	Failure Stress. psia	46666.67	46666.67	46666.67	46666.67	44151.70	41357.29
29							
30	** CALCULATED VESSEL PRESSURE RATING DATA BASED ON USER SPECIFIED WALL THICKNESS						
31	Shell Wall Thickness with Corrosion Allowance. in	0.2500					
32	Inside Radius. in	12.1875					
33	Corrosion Allowance. in	0.0000					
34	Joint Efficiency. 0 to 1	0.85					
35							
36	Maximum Allowable Temperature. F	-20.00	100.00	150.00	200.00	250.00	300.00
37	Maximum Allowable Shell Internal Pressure. psig	287.64	287.64	287.64	287.64	287.64	287.64
38							

flow occurs. This is followed by two phase flow and ultimately as the liquid is mostly depleted, single phase gas flow. This behavior is discussed by Melhem [4] and also verified using actual test data by the Energy Institute [2]. Simpson [12] assumed that the all liquid-venting assumption is conservative and that two-phase mixture behavior is intermediate between the gas-only and liquid-only venting. As shown in Figure , the all-liquid assumption is not conservative and the two-phase flow assumption leads to a larger relief requirement.

In general, the mechanical integrity of the vessel is likely to be determined by this short quasi-dynamic period of time. Most existing STHE relief systems have been historically designed for all vapor venting. The relief areas will be undersized for two-phase venting. The purpose of this quasi-dynamic analysis is to determine if the stress in the vessel will be high enough to cause deformation of the shell considering the low frequency of the initiating scenario.

A first step in this analysis is to confirm the pressure rating of the shell and to provide a failure stress criteria as a function of metal temperature. For this example, the shell pressure rating is confirmed by SuperChems Expert as shown in Figure 10 for the material of construction selected. The ultimate tensile strength is scaled by 2/3 to allow for uncertainties in material properties, corrosion, etc. If the built up internal vessel stress exceeds this criteria at the temperature of interest, then the relief device/system is not adequate for this low frequency scenario and should not be tolerated. If on the other hand, the internal stress reached under two-phase venting is below this limit, an operator can elect to tolerate the risk of deforming the shell but not failing it at the frequency of the tube failure because it is low enough.

Figure 11: Shell failure stress as a function of metal temperature

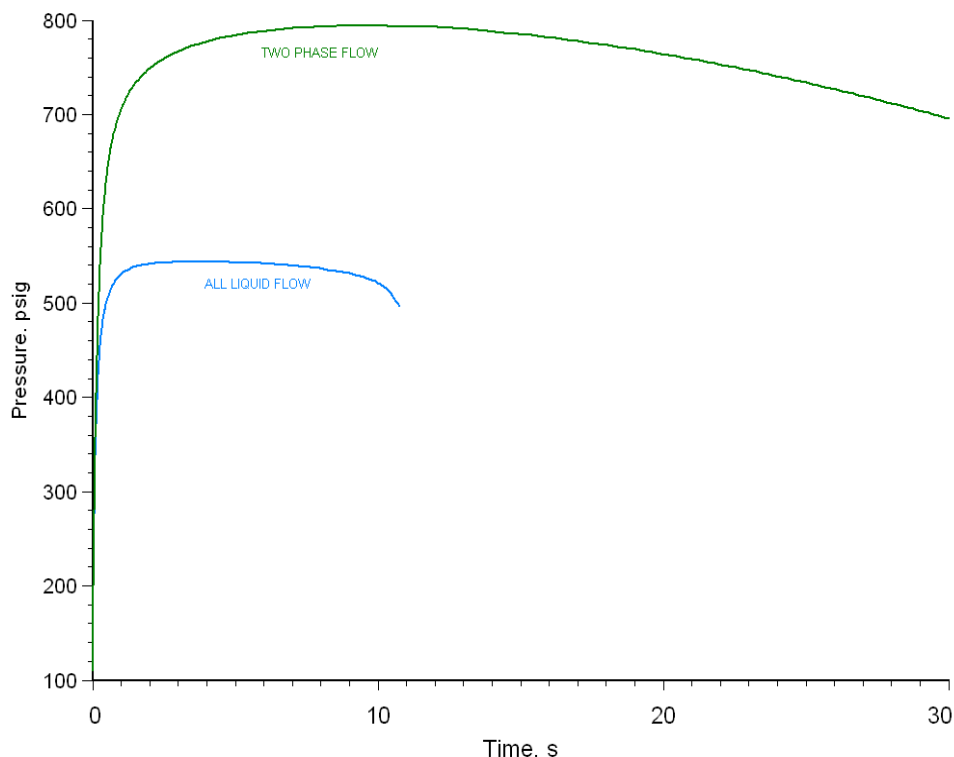


The failure limit decreases with metal temperature as shown in Figure 11 although this is not an issue for this example. This type of criteria is often used in conjunction with dynamic simulation to assess the mechanical integrity of vessels under fire exposure as shown by Melhem [13].

The SuperChems Expert dynamic simulation considers the flow from both ends of the ruptured tube as a function of shell backpressure and performs detailed time dependent mass and energy balances as well as physical and chemical equilibria to determine pressure, temperature, composition, reaction forces, etc. for the shell as a function of time. For illustration purposes, we calculate the time dependent pressure in the shell and the reaction forces at the end of the relief discharge piping for both all liquid flow and two-phase flow. We note that two-phase flow will be homogeneous and there will be no vapor/liquid disengagement because the geometry of most heat exchangers is not suitable for vapor/liquid disengagement. Initially the two-phase flow will be liquid rich as the shell is essentially liquid full. Figure 12 illustrates the pressure history in the shell. The venting is performed through the actual relief piping isometric consisting of the inlet line, rupture disk, and relief discharge piping at every time step. We note that the shell is emptied much faster with all liquid flow, and the pressure is higher with two-phase flow.

The quasi-steady state reaction forces will be higher for two-phase flow in this case because the pressure reached in the shell is higher. Note that SuperChems calculates a time dependent flow impulse ($mu + PA$) at every piping axial location. In order to get the actual reaction force imparted to the entire relief piping, $P_a A$ must be subtracted from the flow impulse at the exit plane of the discharge piping. For liquid and/or sub-sonic flow the net reaction force will be equal to mu_e and

Figure 12: Shell pressure history following tube rupture for all liquid and two-phase flow



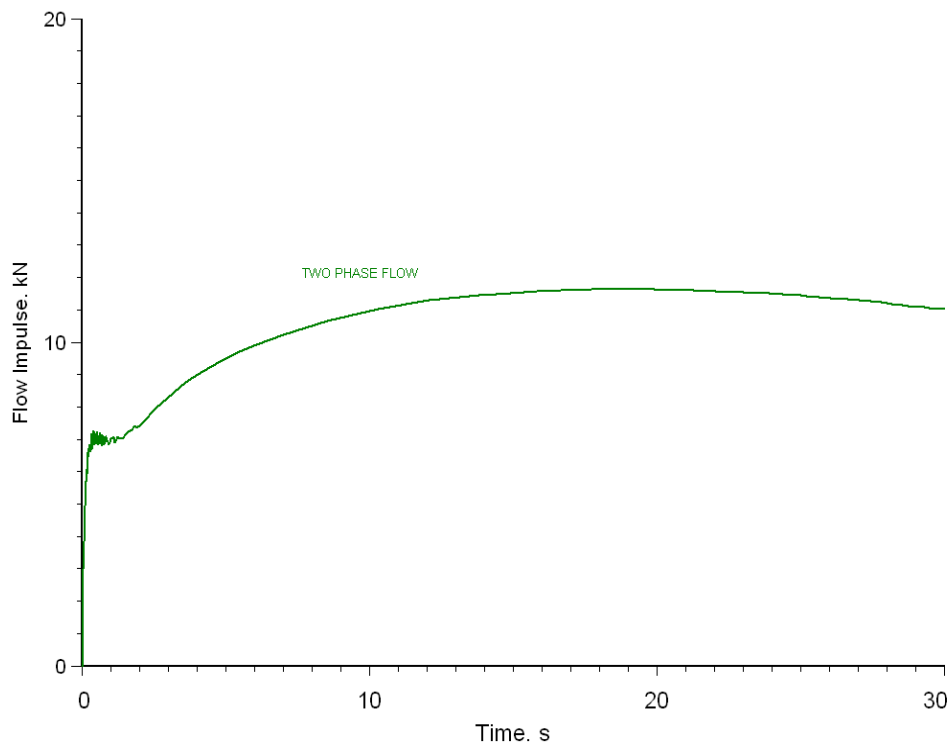
for sonic flow where choking occurs it will be equal to $mu_e + (P_e - P_a)A_e$. This is illustrated in Figure 13.

The relief piping will be subjected to a peak flow impulse of approximately 11.6 kN as shown in Figure 13. However, the exit pressure is choked at 30.2 psig and the exit flow area of the 6 inch pipe is 28.890 in². A value of 5.75 kN would need to be subtracted from the 11.6 kN flow impulse to yield a peak quasi steady reaction force of 5.83 kN. There are utility scripts available to extract this data automatically in SuperChems version 8.2. By comparison,

- A The reflected liquid displacement shell force was calculated at 441.5 kN for 8.9 milliseconds, or as an impulse of 3925 N.s
- B The transient liquid reaction force (without the dynamic load factor) applied to the 6 inch discharge segment of the relief piping was calculated to be 0.37 kN for 4.08 seconds or as an impulse of 1525 N.s
- C The quasi-steady reaction force (without the dynamic load factor) during two-phase venting was calculated at 5.83 kN for 30+ seconds or as an impulse of 174,900 N.s

The relief piping must be analyzed for structural integrity of the supports using the right tools for structural analysis.

Figure 13: Relief piping flow impulse at the exit plane for two-phase flow



11.3 C - Required Rupture Disk Size

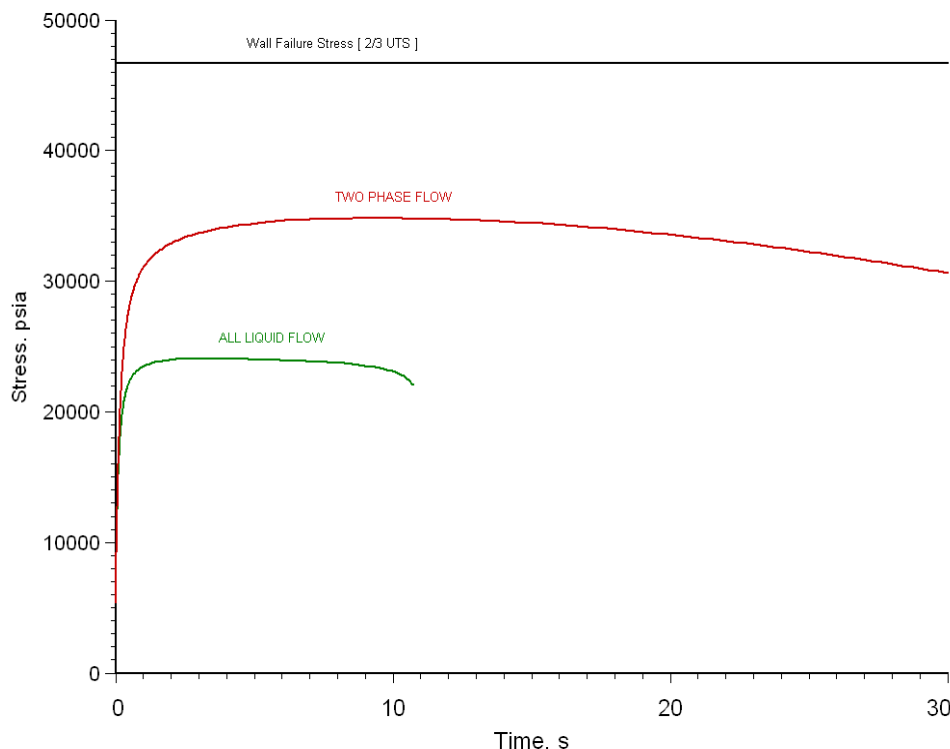
Although the pressure exceeds the corrected hydrostatic pressure in the shell, this does not mean that the vessel is likely to fail. As shown in Figure 14 the built up internal stress in the vessel is below the established failure stress based on $2/3$ UTS. Although the shell is likely to get deformed, the shell is not likely to fail. As indicated earlier, this might be an outcome that can be tolerated if the tube failure frequency is low enough or the risk is low enough.

12 SuperChems Expert Guidance

SuperChems Expert provides several validated and detailed models that can be used to properly analyze a tube failure scenario with efficiency. These models include:

- (a) single and multiphase pipe flow models - These models are used to establish the flow from both ends of the ruptured tube and can account for phase change due to expansion. We typically generate a complete backpressure curve of the flow from each end of the tube and connect to the dynamic vessel flow models to represent the decline in flow entering the shell as the pressure increases in the shell. They are also used to calculate the initial dynamic reaction force on the relief piping associated with all liquid flow upon the initial burst of the

Figure 14: Shell internal stress vs. failure stress at 2/3 UTS



rupture disk by removing the discharge piping as a special case for the analysis. Vibration risk is automatically calculated by these modules as well as PRV stability.

- (b) ideal nozzle model - This model is similar to the pipe models. It can be used to quickly establish an upper bound on the flow from the broken tube with phase change as well as the initial dynamic reaction force to the relief piping.
- (b) sudden flow and valve closure model - This model is used to establish the peak incident loads and load durations associated with the initial liquid displacement in the shell. This model can be used to model cases dealing with any kind of fluid state (gas, liquid, two-phase, supercritical, etc.) from a broken tube striking liquid in the shell side as well as the peak pressures developed by sudden valve closures for any kind of single or multiphase flow. Shocks from high pressure gas flow striking a low pressure gas can also be modeled for the special case when both sources have the same flow diameter, a typical case often encountered in a rupture disk relieving into a common header where other rupture disks are tied into as well.
- (d) dynamic single and multiphase vessel models - These models are used to evaluate the transient pressure buildup in the shell, quasi-steady reaction forces for the relief piping, the required relief requirement, as well as to provide a first screen for potential vessel failure using hoop stress and a user established maximum allowable tensile strength curve as a function of temperature typically set at 2/3 the ultimate tensile strength.

13 Conclusions

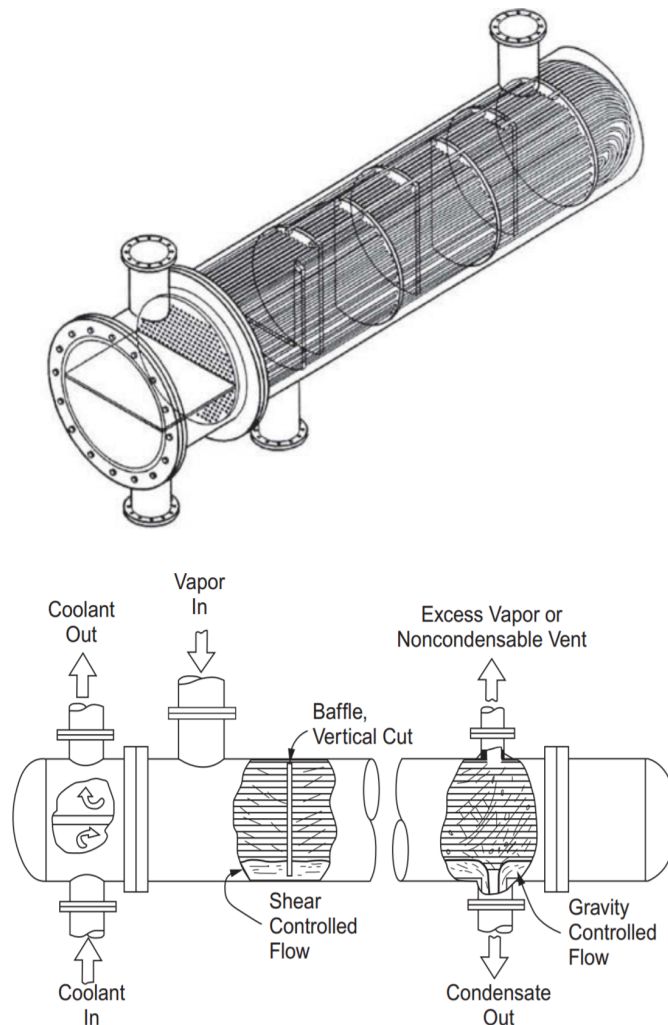
The high pressure ethylene STHE example solution demonstrates that the existing relief system can tolerate a sudden tube rupture and that the shell is likely to get deformed but not fail. The relief system piping is subjected to high reaction forces and the supports should be checked for adequacy for the initial liquid dynamic loads as well as the quasi-steady loads during two phase flow.

This paper demonstrates a systematic work process and methodology to evaluate the risks of potential STHE shell failure when subjected to pressures and loads from a sudden tube rupture. The work process is efficient and detailed. When applied with the right computing tool, such as SuperChems Expert, rapid identification, screening, and ranking of STHE shell failure risks can be performed. This enables operating companies to determine where risk reduction is truly needed and to efficiently utilize resources to implement risk reduction only where needed and effective.

14 Appendix A - Shell Side High Pressure Condition

The analysis presented in this paper considers the high pressure fluid to be on the tube side and the low pressure fluid to be on the shell side. The same methodology can be applied if the situation was reversed where the high pressure fluid was on the shell side and the low pressure fluid was on the tube side. In this case, the tube channel becomes the low pressure side and the tube becomes the high pressure side.

Figure 15: TEMA CFU cross section



When the high-pressure fluid is on the shell-side of the heat exchanger, special considerations of the heat exchanger design and geometry are required to determine the flow path and impact of the moving pressure surge. TEMA² designates heat exchangers with a three letter code based on the front end stationary head type, the shell type, and the rear end head type. AEP designates an exchanger with a channel and removable cover on the front end head, a one pass shell, and an

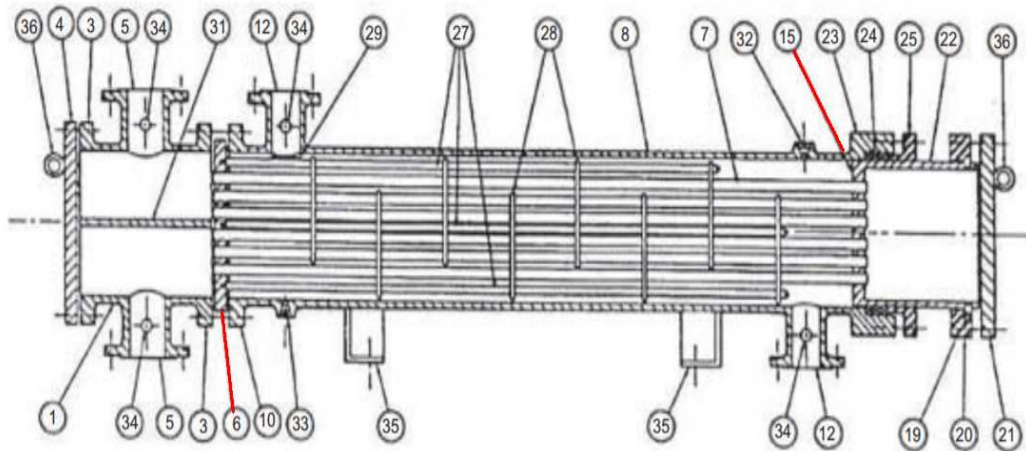
²Tubular Exchanger Manufacturers Association

outside packed floating head on the rear end. CFU designates an exchanger with a channel integral with tubesheet and removable cover, a two-pass shell with longitudinal baffle, and a u-tube bundle.

For illustration purposes, we consider a TEMA AEP design exchanger³ as shown in Figure 15. In the AEP⁴ configuration as shown in Figure 16, for example, there is both a stationary tubesheet (Item 6) and a floating tubesheet (Item 15). When the tube break occurs at the backside of a tubesheet, the flow path from the high-pressure shell to the low-pressure channel and attached piping is through the tube stub remaining in the tubesheet and the longer tube section. The initial incident pressure acts along the length of both channel barrels.

In a CFU type heat exchanger as shown in Figure 17, due to the pass partition (Item 31), the moving pressure will impact the low-pressure channel and be spread along the length of the channel barrel on both sides of the partition.

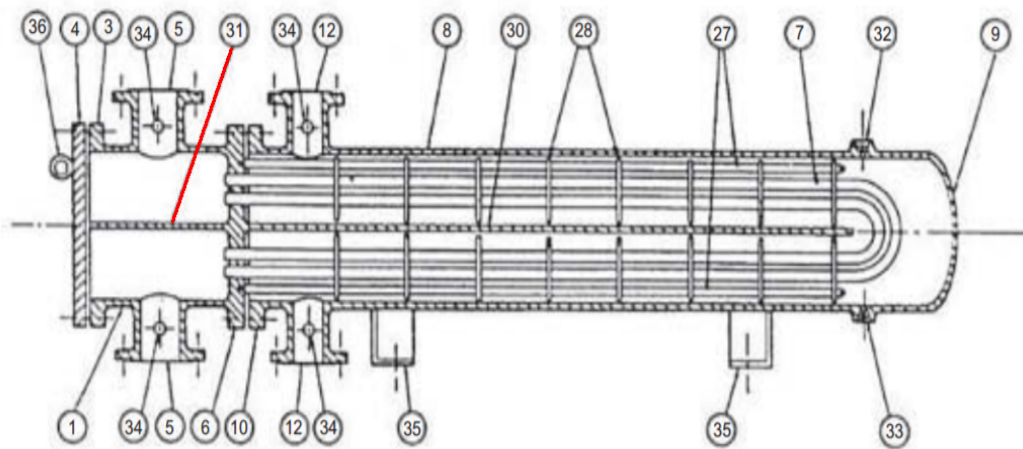
Figure 16: TEMA AEP



³M. Stewart, Lewis O. T., Heat Exchanger Equipment Field Manual, Elsevier, 2013

⁴Standards of the Tubular Exchanger Manufacturers Association, 6th Ed., 1978

Figure 17: TEMA CFU



References

- [1] The Institute of Petroleum. Guidelines for the design and safe operation of shell and tube heat exchangers to withstand the impact of tube failure. Technical Report ISBN 0 85293 286 3, The Institute of Petroleum, 2000.
- [2] The Energy Institute. Guidelines for the design and safe operation of shell and tube heat exchangers to withstand the impact of tube failure. Technical Report ISBN 978 0 85293 757 0, The Energy Institute, 2015.
- [3] Dilip K. Das. How heat exchangers tubes fail. In *4th Annual SuperChems Users Group Meeting, Houston, Texas*, 2010.
- [4] G. A. Melhem. Model the dynamics of heat exchanger tube failure. In *DIERS Users Group Meeting, Reno, Nevada*, 2010.
- [5] John Spouge. New generic leak frequencies for process equipment. *Process Safety Progress*, 24(4):249–257, 2005.
- [6] API. *API Recommended Practice 581 - Risk Based Inspection Methodology*. American Petroleum Institute, 3rd edition, 2016.
- [7] G. A. Melhem. On the estimation of speed of sound and thermodynamic properties for fluid flow and PRV stability. In *DiERS Users Group Meeting*. DiERS, AIChE, April 2016.
- [8] Frederick J. Moody. *Introduction to Unsteady Thermofluid Mechanics*. Wiley, 1990.
- [9] G. A. Melhem, M. Brewer, and M. Porter. The anatomy of liquid displacement and vapor breakthrough. In *12th Global Congress on Process Safety*. CCPS Center for Chemical Process Safety, AIChE, 2016.
- [10] CCPS/AIChE H. G. Fisher and G. A. Melhem (Editors). *Guidelines for Pressure Relief and Effluent Handling Systems*. Wiley, New York, 2nd edition, 2016.
- [11] B. C. Ewan and M. Moatamedi. Design considerations to prevent heat exchanger failure. *Hydrocarbon Processing*, November.
- [12] L. L. Simpson. High pressure gas-filled tubing rupture in liquid-filled heat exchangers. In *Symposium on Safety in Design and Operations of Venting Systems*, number 54D. AIChE, AIChE, 1971.
- [13] G. A. Melhem and D. Gaydos. Properly calculate vessel and piping wall temperatures during depressuring and relief. *Process Safety Progress*, 34(1):64–71, 2015.

About the Author



Dr. Melhem is an internationally known pressure relief and flare systems, chemical reaction systems, process safety, and risk analysis expert. In this regard he has provided consulting, design services, expert testimony, incident investigation, and incident reconstruction for a large number of clients. Since 1988, he has conducted and participated in numerous studies focused on the risks associated with process industries fixed facilities, facility siting, business interruption, and transportation.

Prior to founding ioMosaic Corporation, Dr. Melhem was president of Pyxsys Corporation; a technology subsidiary of Arthur D. Little Inc. Prior to Pyxsys and during his twelve years tenure at Arthur D. Little, Dr. Melhem was a vice president of Arthur D. Little and managing director of its Global Safety and Risk Management Practice and Process Safety and Reaction Engineering Laboratories.

Dr. Melhem holds a Ph.D. and an M.S. in Chemical Engineering, as well as a B.S. in Chemical Engineering with a minor in Industrial Engineering, all from Northeastern University. In addition, he has completed executive training in the areas of Finance and Strategic Sales Management at the Harvard Business School. Dr. Melhem is a Fellow of the American Institute of Chemical Engineers (AIChE) and Vice Chair of the AIChE Design Institute for Emergency Relief Systems (DiERS).

Contact Information

Georges. A. Melhem, Ph.D., FAIChE

E-mail. melhem@iomosaic.com

ioMosaic Corporation

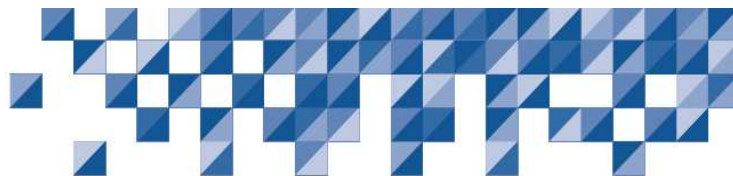
93 Stiles Road

Salem, New Hampshire 03079

Tel. 603.893.7009, x 1001

Fax. 603.251.8384

web. www.iomosaic.com



Offices

Headquarters (Salem)

ioMosaic Corporation
93 Stiles Road
Salem, New Hampshire 03079

Houston Office

ioMosaic Corporation
1900 St James Place, Ste 700
Houston, Texas 77056

Minneapolis Office

ioMosaic Corporation
401 North 3rd St, Suite 410
Minneapolis, Minnesota 55401

Middle East Office - Bahrain

Office No. 161 & 162
Platinum Tower Building No. 190
Road No. 2803, Block 428
Al Seef, Kingdom of Bahrain

Contact Us

www.ioMosaic.com
sales@ioMosaic.com
1.844.ioMosaic

Software Solutions

Process Safety Enterprise®

Effectively manage the reliability, availability, maintainability, and auditability of critical process safety data and PSM elements.

Process Safety Office™

Leverage a fully integrated platform for process safety and risk management.

About ioMosaic Corporation

Through innovation and dedication to continual improvement, ioMosaic has become a leading provider of integrated process safety and risk management solutions. ioMosaic has expertise in a wide variety of areas, including pressure relief systems design, process safety management, expert litigation support, laboratory services, training and software development.

ioMosaic is an integrated process safety and risk management consulting firm focused on helping you manage and reduce episodic risk. Because when safety, efficiency, and compliance are improved, you can sleep better at night. Our over 300 years of combined industry expertise allow us the flexibility, resources and capabilities to determine what you need to reduce and manage episodic risk, maintain compliance and prevent injuries and catastrophic incidents.

Our mission is to help you protect your people, plant, stakeholder value, and our planet. For more information on ioMosaic, please visit: www.ioMosaic.com.

Consulting Services

- Auditing and Due Diligence
- Chemical reactivity management
- Combustible dust hazard analysis (DHA) and testing
- Due diligence support
- Effluent handling design
- Pressure relief and flare systems design
- Facility siting
- Fault Tree/SIL/SIS Analysis
- Fire and explosion dynamics
- Incident investigation, litigation support, and expert testimony
- Liquefied natural gas (LNG) safety
- Pipeline safety
- Process engineering design and support
- Process hazard analysis (PHA)
- Process safety management (PSM)
- Quantitative risk assessment (QRA)
- Risk management program development
- Structural dynamics
- Training

Laboratory Testing Services

- Chemical Reactivity
- Combustible Dust
- Battery Safety
- Specialized Testing